Synthesis of CuS Nanorods: Effect of α-Alanine on their sizes and their applications in solar cell

A Dissertation Submitted to the Department of Chemistry, Quaid-i-Azam University, Islamabad, in Partial Fulfilment of the Requirements for the Degree of

Master of Philosophy

In

Physical Chemistry

By

MUHAMMAD RAMZAN

Department of Chemistry
Quaid-i-Azam University Islamabad, Pakistan (2016)

DECLARATION

This is to certify that this dissertation submitted by **Mr. Muhammad RAMZAN** is accepted in its present form by the Department of Chemistry, Quaid-i-Azam University, Islamabad, as satisfying the partial requirement for the degree of Master of Philosophy in Physical Chemistry.

Supervisor: _____
Dr. Azhar Iqbal

External: _____

Head of Physical Chemistry Section: _____
Dr. Hazrat Hussain

Chairman of Department: _____
Prof. Dr. Mohammad Siddiq

ACKNOWLEGDEMENT

We are thankful to Almighty ALLAH who is the most bounteous and most merciful, and created us as a crown of the creatures in his universe. He not only made us the follower of The Holy Prophet Peace Be Upon Him but also show us the right path of virtue and gave us knowledge to observe the universe, blessed us brilliant mind to make the experiment on his living and non living creature for the betterment of humanity. Our all inventions, discoveries, perceptions and predicts those are depend our struggle and hard work but not possible without his help. We can not only improve, develop and change the world with knowledge but also we can make it peaceful atmosphere for human beings to following the foot step of our ancenters and for-fathers.

I am very grateful to my respected and honourable supervisor Dr. Azhar Iqbal (Assistant Professor Department of Chemistry, Quaid-i-Azam University Islamabad) who encouraged and motivated me to getting my goal within given specific period. May ALLAH bless him whose scientist mind polished my scattered thoughts according to the impartial scientific method. He also took special interest, attentions and concentrations to make me able to complete this research work.

I am thankful to my respected Professor Dr. Muhammad Siddiq (Chairman, Department of Chemistry Quaid -i-Azam University Islamabad) for great, nice assistance and ethical support.

I am very prayed to Dr. Hazrat Hussain (Head of Physical Section) Department of Chemistry Quaid-i-Azam University Islamabad for his kind support to providing me relevant research facilities.

Specially thanks to Professor Dr. Safeer Ahmed whose kindful pieces of guidance were with me in solar cell fabrication and I-V measurement.

I would like to thankful to all staff, faculty members and all respected teachers of physical section who support me in each and every think and thin throughout in my M.Phil section.

I also grateful to all of my lab fellows especially Nasreen Bibi, Zumaira Siddique, Saira Shakoor and Shumaila Saeed for their great company and cooperation in lab during my research work.

My further prays are for all friends and colleagues either they belong to Quaid-i-Azam University or another institute who supported me what so ever I had required, Samar Munir, Saira Fyaaz, Muhammad Adeel, Muhammad Faheem, Babar taj, Muhammad Soahil, Zawar

Hussain, Ali Raza, Muhammad Ajmal, Mehtab, M. Khurrm, Ansir Mehmood, Majid Hussain and Muhammad Sami were special of them. May Almighty Allah bless his blessing to all of those, who helped and supported me in throughout my M.Phil section.

Muhammad Ramzan

CONTENTS

List of Figures

List of Tables

Abstract

Semiconducting nanorods, whose particle sizes are in 1-100 nm range, have very unusual properties. The quantum dots have band gaps that depend in a complicated fashion upon a various number of factors. First of all we synthesized CuS nanorods through the co- precipitation method. The confirmation of the CuS synthesis is done by the FTIR spectroscopy. The further confirmation that CuS exists in the form of quantum dots is done by X-ray diffraction (XRD) and scanning electron microscopy (SEM). Optical studies are carried out by steady-state fluorescence and UV-Visible techniques. XRD patterns further suggest that CuS nanoparticles are grown in hexagonal crystal structure with the average crystallite size ~15.6 nm and by increasing the concentration of α-Alanine the size is decreased. SEM images suggest that the CuS nanoparticles have been agglomerated and appeared in the form of rod shape. The quantum dots sensitized solar cell is fabricated by spin coating method. Finally the voltage current measurements are done by solar simulator, which show the V_{oc} 0.77 & 0.79 V, J_{sc} 0.00258 & 0.00273 Acm^{-2} and the efficiency (%) 0.97and 1.2 for the CuS nanorods containing the 1mM and 51 mM of α-Alanine respectively.

.

Chapter 1

Introduction

1.1 Nanotechnology

Nanotechnology is a blend of two Greek words prefix “nano” refers to a billionth and the word technology. As a conclusion, the size below 0.1μm or 100 nm is usually regarded as a nanoscale and is used in nanotechnology or nanoscale technology. The nanoparticles, especially below the 5 nm size have considerably different considerable properties as compared to larger particle size.[1]

Nanotechnology is known as emerging technology due to many well established advanced products having the completely different characteristics and functions in different fields of applications. Nanotechnology is a vast field having large applications in biotechnology, biochemistry, communication technology, metrology, medical technology and has also a various innovations and industrial applications.[2] There are also many different fields in which nanotechnology having significant applications such as cosmetics, electronics, chemical engineering, pharmaceutics, environmental science, food industry, optics, precision mechanics and energy productions. More than 50,000 nanotechnology articles publications annual at world level in current years prove that nanotechnology is a vibrant and promising field.[3]

Many serious problems such as fatal diseases, energy adequacy or climate change have been solved with the help of nanotechnology methods. With the enhancing competitiveness of our industry there are also a lot of important products in different fields that have made really a positive change in the citizen’s life with the improving medical, electronics and many other fields.[4] Nanotechnology creates and uses structures that have novel properties because of their small size. There are many new different fields of research which have a more interest due to the nanotechnology applications. The fatal diseases such as brain tumors and Alzheimer’s disease are treated with new medical technology. The nanoscale components have been used for the constructions of computers and their performance and efficiency depend on shrinking the nanomaterials size. Nanomaterials such as carbon nanotubes, quantum dots, fullerenes, quantum wires, nanocomposites and nano fibers due to the inimitable properties they have new applications in different fields. The range of commercial products available today is very wide, including metals, ceramics, polymers, cosmetics, sunscreens, smart textiles, paints, electronics and varnishes. On the other hand, new techniques and instrumentation have to be build up in arrange to increase our understanding and information on their properties.[4]

Due to potential effects of nanomaterials on health and possible environmental impacts, it must be examined. At world level there must be strongly recommendation for safety evaluation of nanoscience products by the specific guidance documents. Enormous ambitions are paid to nanotechnological expansions in the modern medicine. The properties of nanoparticle depend on their sizes, with changing the size their properties also change. The chemical composition, which basically dictates the native toxic properties, so small size shows to be a principal indicator for extreme toxic effects of particles.[4, 5]

1.2 Nanorods and Quantum Dots

Nanorods can be produce by the different direct chemical methods. The combination of the ligands act as the shape control agents and also bond to different surfaces of the nanorods with the different strengths. As a result this allows growing different faces of the nanorods at the different rates. The diameter range for nanorods is 1-100 nm and for quantum dots is 2-10 nm. Nanorods, quantum dots, nanoparticles and nanocrystal are classified as nanostructures. With the decrease in dimensions of nano materials, the surface of nanostructures starts to exhibit new and interesting properties.[6] Nanorods are most motivating and attracting nanomaterials that have been discovered. Nanomaterials have more important and valuable original properties such as band gap that is the result of quantum confinement into three dimensions. The variation in the size of the nanomaterials is observed due to the variation in the absorption spectrum. The blue-shift occurring in the absorption spectrum shows that the decreased in the size of nanoparticles. There is an inverse relation between the size of nanoparticles and band gap. If the band gap is more its mean small the size of nanoparticle and vice versa.[7] Quantum mechanical principle is followed by the quantum dots and nanorods. Quantum dots (QDs) belongs to a division which is famous as engineered nanoparticles (ENPs). There are numerous fields such as solar energy, medical treatment, drug biosensing, light-emitting diodes and diagnostic treatments in which nanorods are used. Nanorods have many important properties such as high photo stability and tunable size. In the periodic table the elements of groups IV–VI, II–VI, or III–V are normal used for the composition of nanocrystal.[7, 8] In 1980 by Russian physicist Ekimov the history of quantum dot was initiated by earliest discovery in crystal of glass. Quantum dots also known as zero dimensional because it is so tiny particle and its mass concentrate only on a single point. They are semiconductors crystals in nature and the band gap of quantum dots is larger as

contrast to bulk material structure. This bridge of band gap between bulk material structure and nanostructure is very important due to this they have a lot applications in electronics and biology field.[9]

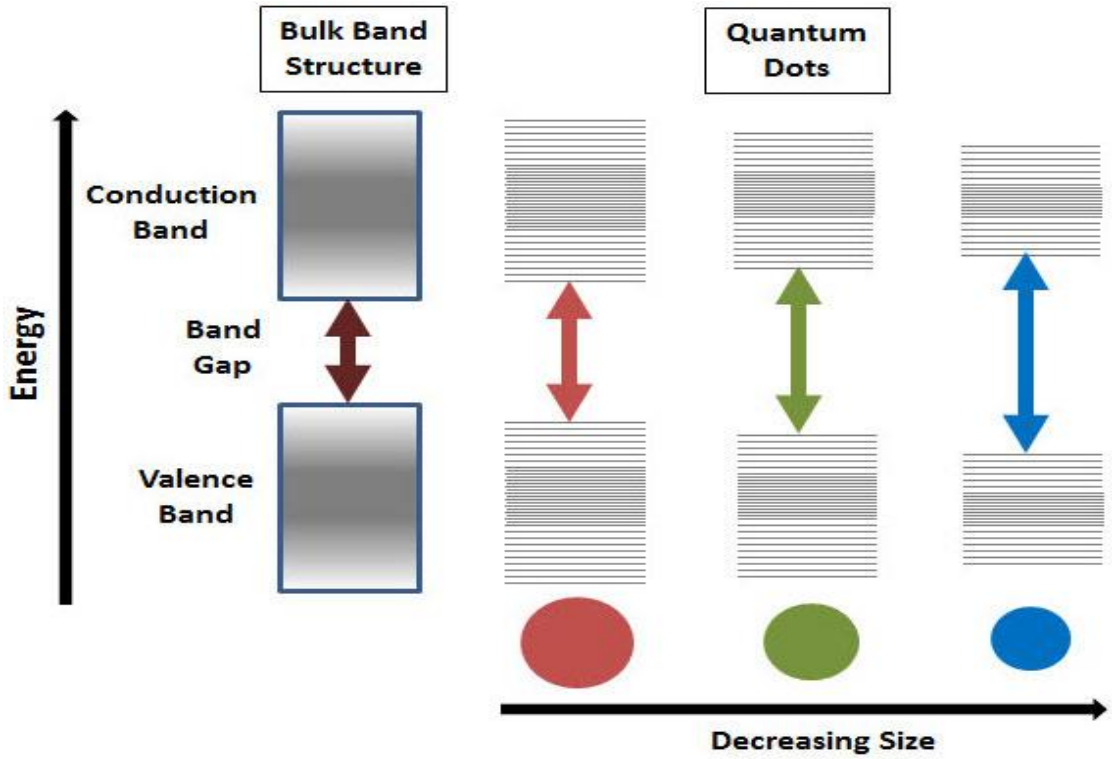

Figure1.1 Relationship between band gap and size of quantum dot.[10]

1.3 Nanomaterials and Band Gap

The energy separation of the conduction and valence band is the most important feature of the semiconductors. This energy is frequently known as the band gap and can be narrated to the physical property which is known as exciton Bohr radius.[11] An exciton is fundamentally a pair of electron-hole. When any electron is excited from valence band (VB) to the conduction band (CB). The static Coulomb force is present which held the electron and hole together. Quantum dots are basically nanostructure material having comparable all dimensions with the value of exciton Bohr radius. Principally the exciton Bohr radius explains how great a crystal should be made until the value of its energy gaps may be delighted as continuous. The size of the crystal and the energy gap of the particle are inversely proportional to each other, the size is reduced by increasing the energy gap and this leads towards the shorter wavelengths in the absorption lines. L.E. Brus recommended a model "particle in a box" that explains the relationship of nanocrystal size with the band gap.[12]

The formulated form of purposed model is given below

$$Eg_{(QD)} = Eg_{(bulk)} + \frac{h^2}{2R^2}\left(\frac{1}{m_e'} + \frac{1}{m_h'}\right) \quad \textbf{(1)}$$

Wherever

h = The Planck's constant, R = Radius of the nanomaterials, m_e= The effective mass of an electron

m_h= The effective mass of an hole , $Eg_{(QD)}$= Band gap energy of the quantum dot

$Eg_{(bulk)}$= Band gap energy of the bulk

This model obviously justifies that a size diminution of nanocrystal leads to the blue-shift of the absorption spectrum. The equation (1) expresses that by increasing the band gap energy the decrease in size of particle is observed. Consequently blue shift is appeared in absorption spectrum at further lower wavelength and the size of nanorods will be reduced.

1.4 Types of Semiconductors

On the basis of band gap, semiconductors are divided into two types which are direct and indirect band gap semiconductors.

1.4.1 Direct Band Gap Semiconductors

Band gap is the minimum energy difference from the top of a valence band to the bottom of a conduction band. Band gap is classified in to two types. First type in which top and bottom of the valence and conduction band respectively take place at the alike value of momentum which is called direct band gap. The schematically representation of direct band gap is given below in figure 1.2.

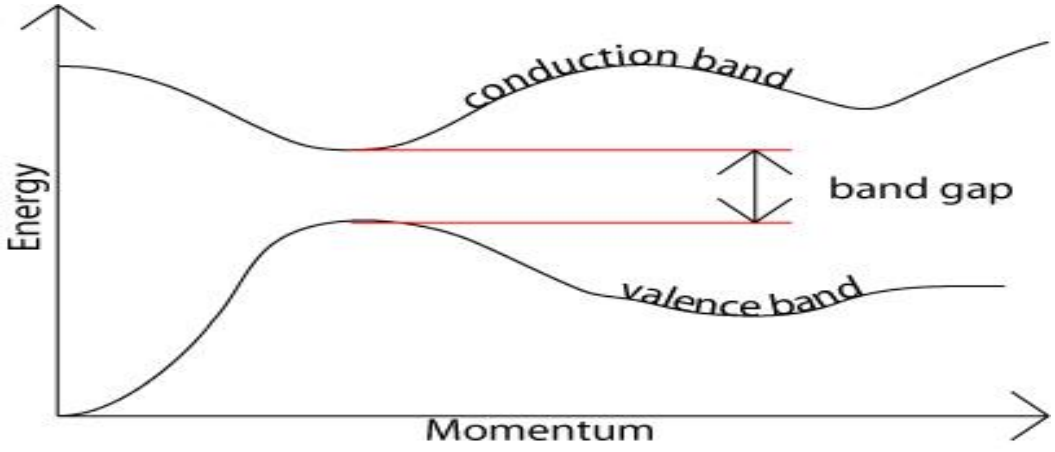

Figure 1.2 Direct Band Gap Semiconductors.[13]

1.4.2 Indirect Band Gap Semiconductors

The other one is indirect band gap semiconductor in which the top of valence band and the bottom of conduction band does not occur at the similar value of momentum, as given below schematically in the figure 1.3.

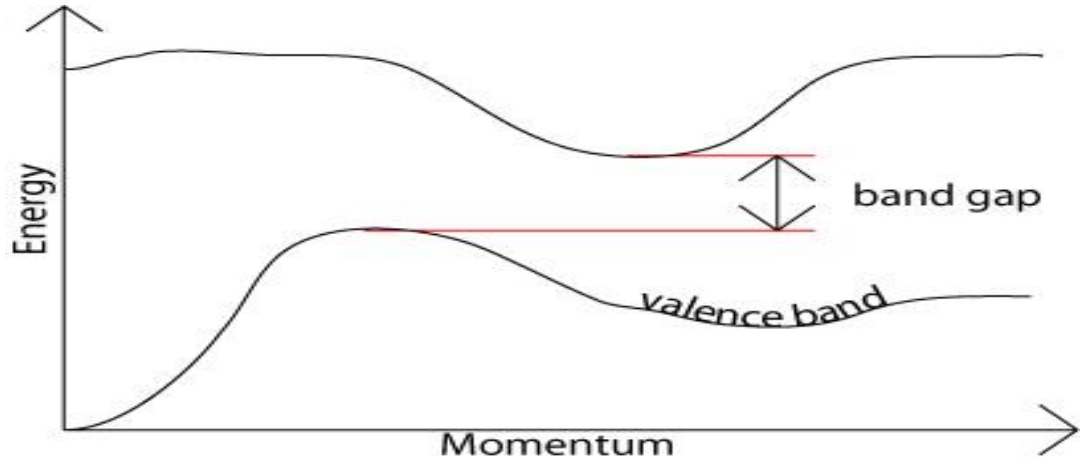

Figure1.3 Indirect Band Gap Semiconductors.[13]

By applying tensile strain we can obtained the trasition that occur from indirect to dierect band structure, in different bands the position of energy changes differentially being a function of strain which is present in each layer.[14] For an efficient optical source and room temperature efficient optical silicon photonics we can use direct band gap semiconductor germanium. Several approaches in literature have been suggested to gain a germanium semiconductor having direct band gap. Thick 'Ge' film having 10 nm thickness which is grown on InGaAs layer having greater lattice constant as contrast germanium showed more than 2.33% biaxial strain tensile.[15] From mechanically bended nanomembrane more than 1.78% biaxial tensile strain was obtained.[16, 17] The Direct band gap has accomplished by micro patterning of germanium on to silicon and shifting uniaxial strains equal to 5.7%. We can also get direct band gap material such as germanium by alloying it with tin.[19-21]

Each photon having the energy (E) has the value of momentum p = E / c, in the expression c indicate velocity of light. A photon having energy equal to band gap can easily create an electron hole pair in a semiconductor which has direct band gap because there is no more need of momentum to an electron. For the production of an electron hole pair in a semiconductor which has indirect bang gap ,there necessity an electron undergo considerable change in its momentum value by a photon having energy E_g. In direct band gap semiconductor there is more efficient recombination process as compare of indirect

band gap semiconductor. As an answer of such thoughtfulness, a gallium arsenide and some other semiconductors (having direct band gap) are mostly used to formulate LEDs optical devices and more efficient semiconductor lasers, for these important applications a Germanium is considered an ideal applicant to get a laser source on the silicon. The bulk Germanium is a example of indirect band gap semiconductor.[13]

1.5 α-Alanine

α-Alanine is an amino acid having the two functional group one is basic amine group and other is acidic carboxylic acid group. It acts as Capping & Stabilizing agent. It also have two carbon skeleton one is present in form of carbonyl carbon and other is present in the form of carbon chain.

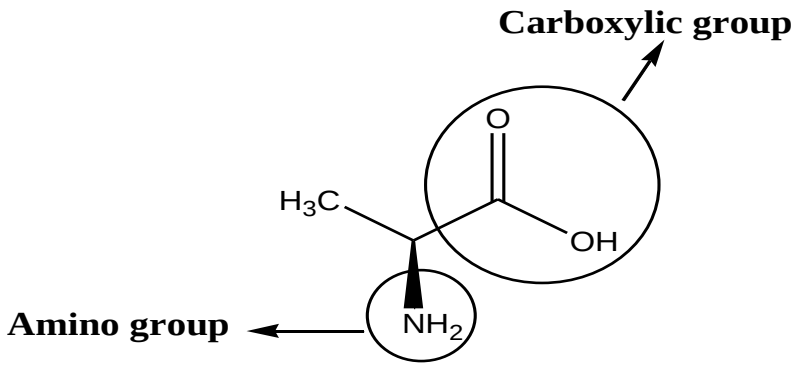

Figure 1.4 α-Alanine

In an amino acid an internal transfer of the hydrogen ion is taken place from the -COOH group to $-NH_2$ group and consequently an ion is produced having both the negative and positive charge which is known as zwitterion. A zwitterion is overall electrical neutral with two separate positive and negative charges.[22-24] Zwitterion is pH sensitive it can exist in anionic as well as in cationic form. On increasing the concentration of acidic solution or decreasing the P^H vale it exist in the form of cation on the other hand by increasing the value of P^H or by adding the alkali to an amino acid solution it exist in the form of anion.[25, 26]

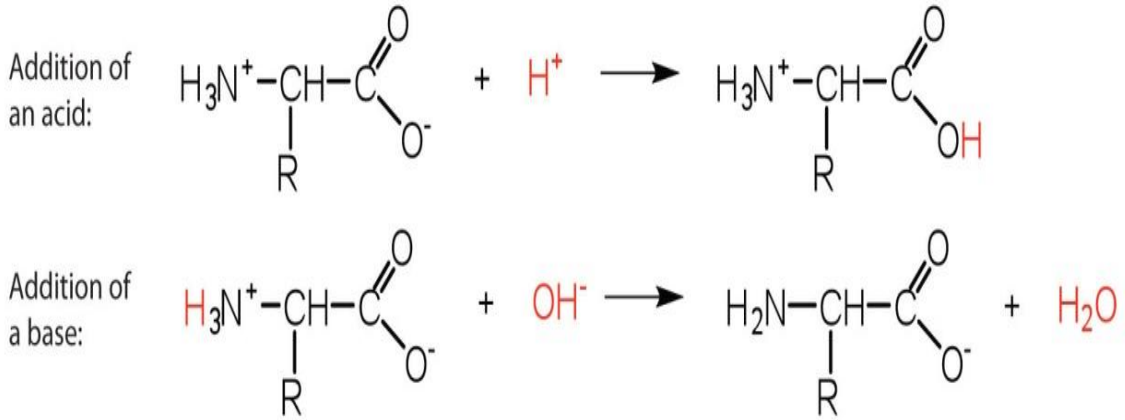

Figure1.5 pH value effect on zwitterionic form.[27]

1.5.1 General Characteristics of α-Alanine

Generally amino acid are optically active and having the property of dissociation in aqueous solution. The solubility of amino acids is highly variable in water solvent. Due to the polar characteristics of an amino acid its solubility is not very good in different organic solvents. Approximately in ether all the amino acids are insoluble. Merely cytosine as well as praline is reasonably soluble in the ethanol solvent (At 19 ^{0}C) but the tryptophan is sparingly soluble in it. Mostly amino acid are spectroscopically active such as Mass spectroscopy, Infrared spectroscopy, UV-Visible spectroscopy and nuclear magnetic spectroscopy. The amino and carboxyl groups of an amino acid are responsible for its reaction specificity.[28-30]

1.5.2 Binding sites and Effect of pH on α-Alanine

It is pH sensitive it can exist in anionic, cationic as well as in zwitterionic form as given in the figure 1.6. At the one pH value it exists in zwitterionic form and anionic form in basic solution having pH value 10.

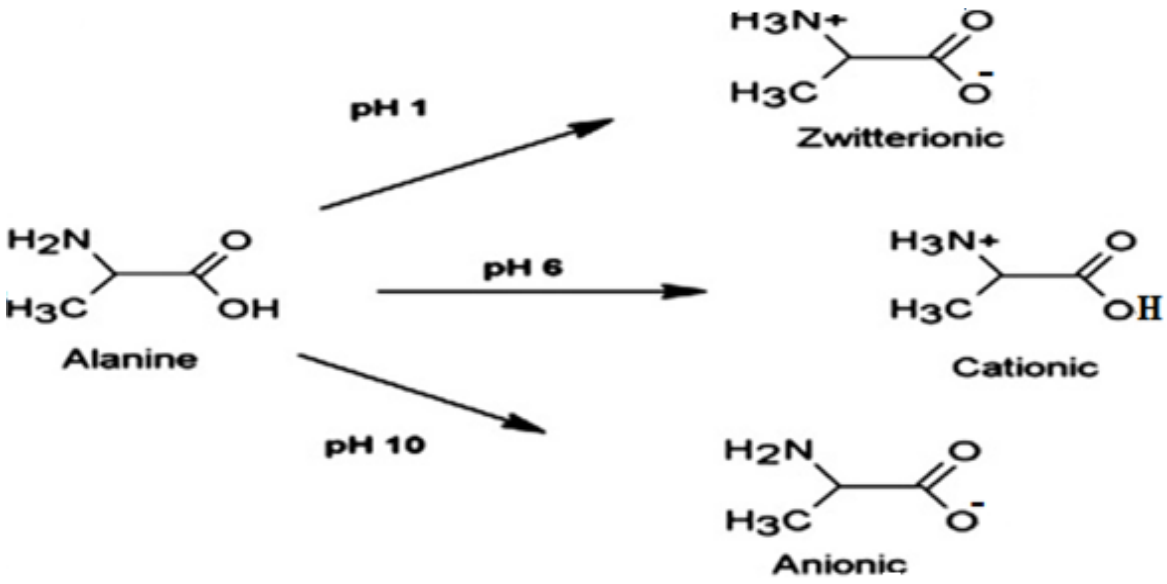

Figure1.6 Effect of pH on α- Alanine.[31]

On the basis of nature of solution there are two binding sites of α-Alanine as shown in the figure 1.7. In the acidic solution α- Alanine has $–NH_3^+$ as binding site but in the case of basic solution the binding site is $–COO^-$.

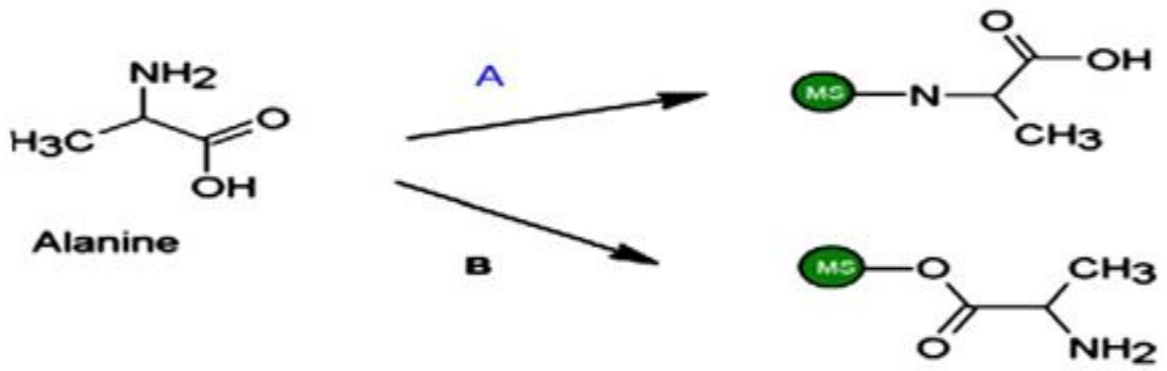

Figure1.7 Binding sites of an α-Alanine.[31]

1.5.3 Physical Interaction of α-Alanine with CuS Nanorods

The α-Alanine has two binding sites which are so sensitive for the pH value of solution. In acidic and basic media the α-Alanine has different binding site which can physical interacts with the CuS nanorods. For one CuS the two α-Alanine molecules required for the proper capping ability. In the basic media the physical interaction between binding site of α-Alanine and CuS nanorods are shown in the figure 1.8.

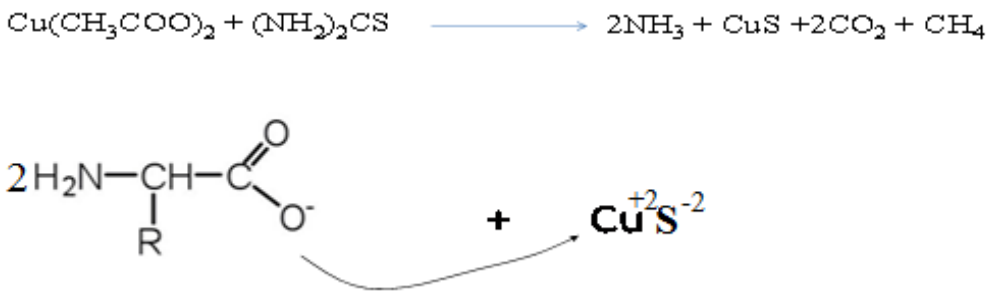

Figure 1.8 Physical Interaction of α-Alanine with CuS Nanoparticles

1.6 Cu_xS Nanorods

Nanoparticles have novel properties such as magnetic, structural, electrical, and optical etc.[32-34] Copper sulphide nanomaterials have reasonably complex crystal structure and chemistry with the formation ability of secondary- stochiometric compounds Cu_xS ($2 \geq x \geq 1$).[35] Copper sulphide can exist in different stable and unstable forms such as copper-poor CuS (covellite) and copper-rich Cu_2S (chalcocite) respectively. There are some other phases such as $Cu_{1.8}S$ (digenite), $Cu_{1.94}S$ (djurleite) and $Cu_{1.75}S$ (anilite).[36-38] Some phases such as $Cu_{1.96}S$, $Cu_{1.8}S$ and $Cu_{1.75}S$ are mostly used for the formation of metastable phases.[39] As CuS has broad applications in different photovoltaic device major one is the solar cell due to the P-type material nature. CuS can display its potential in the range of visible region.[40] Copper sulphide has conductivity which is because of the copper vacancies. Its conductivity decreases from copper-poor CuS phase to copper-rich Cu_xS. CuS and Cu_2S phases exhibit different band gaps value 1.7 and 1.2 eV respectively. While some other phases Cu_xS (x=1.94, 1.8 and 1.75), exhibit band gaps value from 1.05 to 1.96 eV. The covellite (CuS) is the type of I–VI semicondoctor.[41]

1.7 Solar Energy and Nanotechnology

Today solar cell source is too expensive for the production of electricity on large scale. Potential progressions in nanotechnology can also unlock new doors to creation of inexpensive and the slightly well-organized photovoltaic cells. On striking the light with the cells, the absorption of energy is occurred. By the absorption of light energy the excitation of electron from valence band to conduction band occur. Through the absorbed energy the electron knocks out and allowing to flow. By inserting many impurities such as boron and phosphorus to the silicon an electric field may be established. Due to the flow of electron in one direction this type of device is working as a diode.[42] There are two major drawbacks in the usual solar cells: first one is the low efficiencies equal to ten

percent. The second one is they are so costly to construct. The disadvantage of low efficiency is almost indispensable with the type of silicon solar cells due to the inwarding photons should have the exactly energy known as band gap energy, to the tap out number of electrons. If photon has less energy as compare to band gap energy then it will be passed through. If it has the more energy as compare to the band gap energy, then the extra energy will be dissipated as heat.[43] The efficiency of the solar cell can be increased with the help of nanotechnology. The efficiency of the photovoltaic cell will be increased with nanotechnology. A chemist at the University of California, Berkeley, have been discovered inexpensive construct mode of plastic solar cells having efficiency near about equal to 1.7 percent.[44] The nanorods absorb the light of a particular wavelength due to this they behave as wires. These electrons run through nanorods until they reached counter electrode and they will be combined to produce current. This kind of cell is less costly to fabricate than conventional. These plastic cells cannot make from the silicon which is very expensive. Manufacturing of this kind of cells does not necessitate expensive tools as in usual silicon solar cells. Instead, the plastic cells are easily fabricated in beaker. Another important characteristic of these type of solar cells is to absorb a variety of wavelengths of radiations by this feature the efficiency of solar cell can be increased.[45]

1.8 Solar Cell and Photovoltaic Effect

Solar cell is also known as the photovoltaic cell. It converts the light energy directly in to electricity and is designed to capture the energy from sunlight. Photovoltaic effect is physical or chemical phenomenon that creates the electric current or voltage by light exposure in a material. First time in 1839 Alexandre-Edmond Becquerel observed the photovoltaic effect. In 1946 first time the current silicon solar cells were invented by Russel Ohl.[46] In the early days photovoltaic cells are the thin silicon wafers which are used for the transform of sunlight energy into the current.[47] Each cell has been constructed by the two dissimilar p-type and n-type layers of the semiconductor material. In this deal of the structure, when the photon of adequate energy imposes on p-type and the n-type junction, one electron is expelled by getting energy through striking photon and also it goes from n-type to p-type layer. It generates an exciton (electron- hole pair) in route and as a result electrical current is produced.[48] Many type of materials are used for photovoltaic solar cells mostly in the silicon solar cell such as cadmium-telluride, copper indium gallium sulfide and copper indium gallium selenide.[49-53]

1.9 Solar Cell Generations

On the basis of the used materials, there are various classes of photovoltaic solar cells as described in the following figure 1.9.

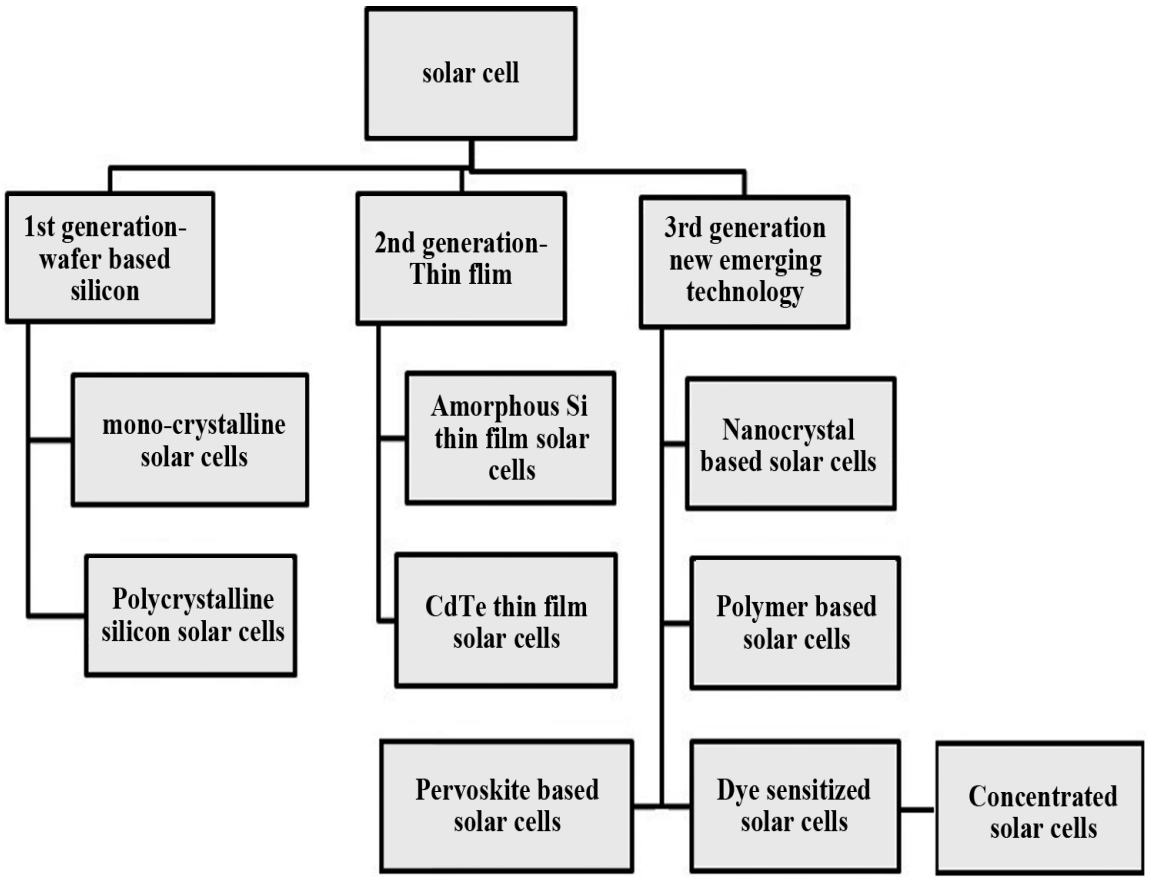

Figure 1.9 Various types of solar cell technologies and its generation.[54]

1.9.1 First Generation Solar Cells

As it is discussed previously, first generation of the solar cells is formed by silicon wafers. This is elderly and accepted technology with having greater power efficiencies. There are further two types of silicon wafer first one is mono-crystalline silicon solar cell and other is the poly-crystalline silicon solar cell.[52]

1.9.1.1Monocrystalline Solar Cells

Monocrystalline silicon is the foundation for silicon chips which are employed in nearly all electronic tools today. Mono-Si also acts as photovoltaic and the light absorbing substance in the construction of the solar cells. It consists of the silicon in which crystal network of complete solids are continuous, constant to its ends, and liberated from any grain limitations.[54] Mono-Si may be fabricated intrinsic, having only remarkably pure silicon and containing very minute quantities of the other essentials to amend its

semiconducting properties. Most silicon monocrystals has been grown by Czochralski process. All These cylinders have sliced into slim wafers of only some hundred microns for advance processing. Single-crystal silicons are possibly the most imperative technological material from last only some decades. Due to its accessibility at affordable cost is vital for the enlargement of electronic machine. Monocrystalline silicons are different from other allotropic appearances such as non crystalline amorphous silicon which is used in the thin-film solar cells and also polycrystalline silicon that contains of small crystals which are known as crystallites.[56]

1.9.1.2 Polycrystalline Solar Cells

Polycrystalline silicon solar cells (polysilicon or poly-Si) have high purity. Polycrystalline silicon is used as unrefined material in many photovoltaic and electronics industries. Polysilicon has been manufactured from the metallurgical grade silicon by means of chemical purification method which is known as Siemens process.[55] This process occupies distillation of explosive silicon compound and at the high temperature decomposition of it into silicon. A rising and alternative method of modification uses the fluidized bed reactor. The polysilicon fashioned for electronics industry restrains less impurity levels than the single part per billion (ppb). A few companies of Japan, China, Korea, Germany and United States reported for the most of the worldwide construction near about more than 230,000 tons in 2013.[57] Polysilicon feedstock bulky rods frequently broken down into large pieces of the specific ranges and packaged in the unsoiled rooms earlier than shipment is straight cast into polycrystalline submitted to the recrystallization method to develop single crystall boules. Multisilicon contains of small crystals, which is called crystallites with having the distinctive metal chip effect. The polysilicon and the multisilicon are mostly used like synonyms. Polylcrystalline mostly refers to the crystalls greater than 1 mm. The polycrystalline solar cell is the mainly general sort of solar cells. According to the estimation near about 5 tons of multisilicons are needed to fabricate one megawatt of usual solar modules. Multisilicon is different from the amorphous and monocrystaline silicon solar cell.[58]

1.9.2 Second Generation Solar Cells

Majority of thin film solar cells are second generation of the solar cells. They are most inexpensive in contrast to first generation of the solar cells. First generation of solar cells have light capturing films with 350×10^{-6} m thickness. But in the second generation solar cells have very slim light capturing layers of the order 1 μm thickness.[55]

1.9.2.1 Thin Film Solar Cell

The thin film solar cell (TFSC) is also known as thin film photovoltaic cell (TFPV). It belongs to the second generation of solar cell. It is made through one or more thin layers by depositing on each other or it is also made by depositing thin film of the photovoltaic material on the surface of a substrate such as metal, glass and plastic.[59] The thickness of thin film changes from nanometers to ten micrometers. Due to this thin film cells behave like flexible and lesser in weight. It is also used in photovoltaics and photovoltaic glazing material for the lamination onto windows. The thin film solar cells are inexpensive but less competent as compare to usual silicon technology. However this type of solar cell appreciably improved greater than years and efficiency for the CdTe nanoparticle are at the present beyond 21 percent related to multicrystalline silicon.[60] In spite of these enhancements market-share of thin-film never reached more than 20 percent in the last two spans. They have been declining in recent years about 9 percent of worldwide photovoltaic installations. Other thin-film technologies, that are at rest in an early stage of current research or with restricted commercial availability, are frequently classified as up-and-coming or third generation photovoltaic cells and include, polymer solar cells ,organic, dye-sensitized, as well as quantum dot, micromorph copper zinc tin sulfide, nanocrystal and perovskite solar cells.[61]

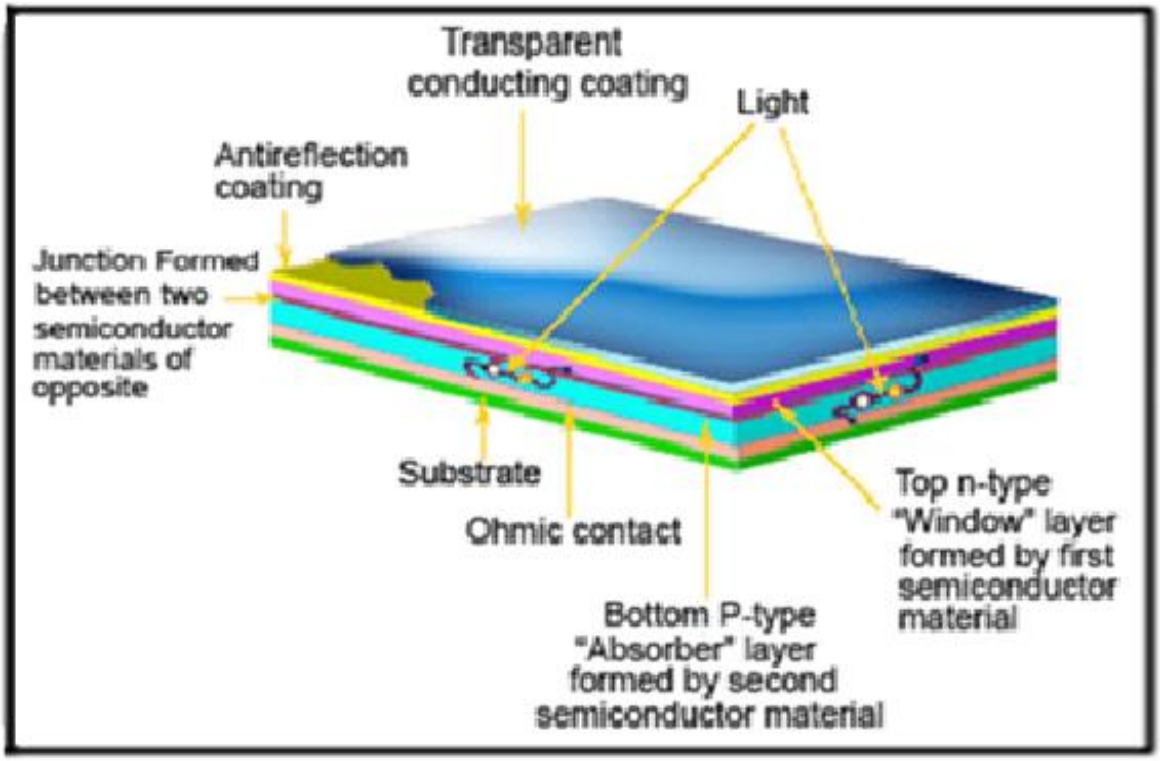

Figure 1.10 Structure of thin film solar cell.[52]

1.9.3 Third Generation Solar Cells

The third generation cells are recent developed techniques. Further classification of third generation solar cells are concentrated solar cells, polymer solar based cells, nanocrystal based solar cells and the dye sensitized solar cells.[54]

1.9.3.1 Dye Sensitized Solar Cell

Dye Sensitized solar cells (DSSC), also known as dye sensitized cells (DSC), belongs to the third generation solar cells that changes the visible light into the electrical energy. The dye sensitized solar cell is a low-cost solar cell. It is based on a semiconductor formed between a photo-sensitized anode and an electrolyte, a photochemical system The modern form of a dye sensitized solar cell, also known as the Grätzel cell, was originally co-invented in 1988 by Brian O'Regan and Michael Grätzel at UC Berkeley.[62] This work was later developed by the aforementioned scientists at the École Polytechnique Fédérale de Lausanne until the publication of the first high efficiency DSSC in 1991 Michael Grätzel has been awarded the 2010 Millennium Technology Prize for this invention. The DSSC has a number of attractive features

- It is simple to make using conventional roll-printing techniques.
- It is semi-flexible and semi-transparent due to which it is used in a variety of ways. In which the glass-based systems not applicable.
- Most of the materials used in DSSC are low-cost.

In spite of these advantages DSSC has a lot of disadvantages and cannot be eliminated. Number of expensive materials, particularly platinum and ruthenium.[63] The liquid electrolyte presents a serious challenge to making a cell suitable for use in all weather. Electrolyte solution contain volatile organic compound which are hazardous to human health and the environment. Liquid electrolyte also has temperature stability problem when temperature come down electrolyte may be frees and when temperature goes up it may be evaporated. Another problem is that most of the dyes degraded when exposed to the UV light. The conversion efficiency of DSSC is less than the best thin-film cells, but its price to performance ratio is good enough to allow them to compete with fossil fuel electrical generation.[64]

The titanium dioxide is white semiconductor that is not sensitive to the visible light. Titanium particles have to be sensitized with a layer of the dye molecules that absorb light in the visible spectrum. Simply DSC composed by order of conductive glass-semiconductor (TiO_2) dye (dye) counter-electrolyte-electrode (pt).[64] How it works,

photon derived from sunlight absorbed by Dye (coloring) and then generated electron. Electron will move quickly to the semiconductor, and then passed to the counter electrode, after which the electrons move through the electrolyte solution (redox processes), and back again to this dye as shown in figure 1.11 (b).

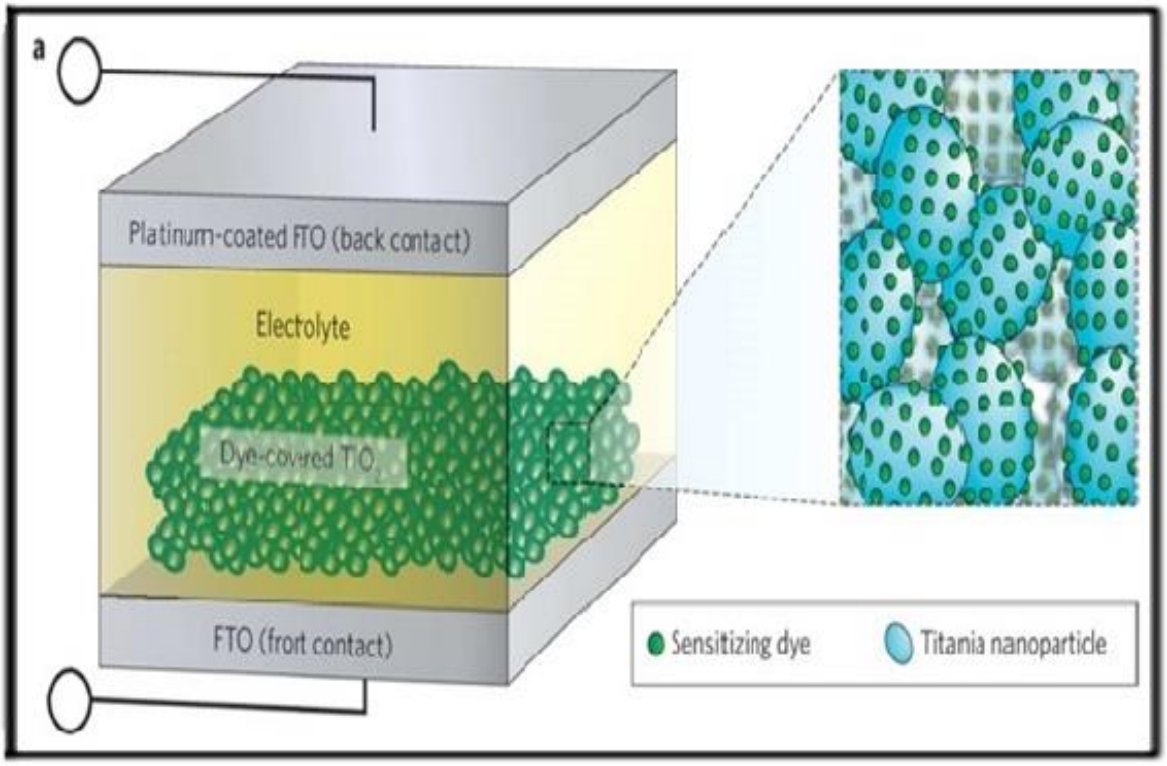

Figure 1.11 (a) Component of dye-sensitized solar cell.[52]

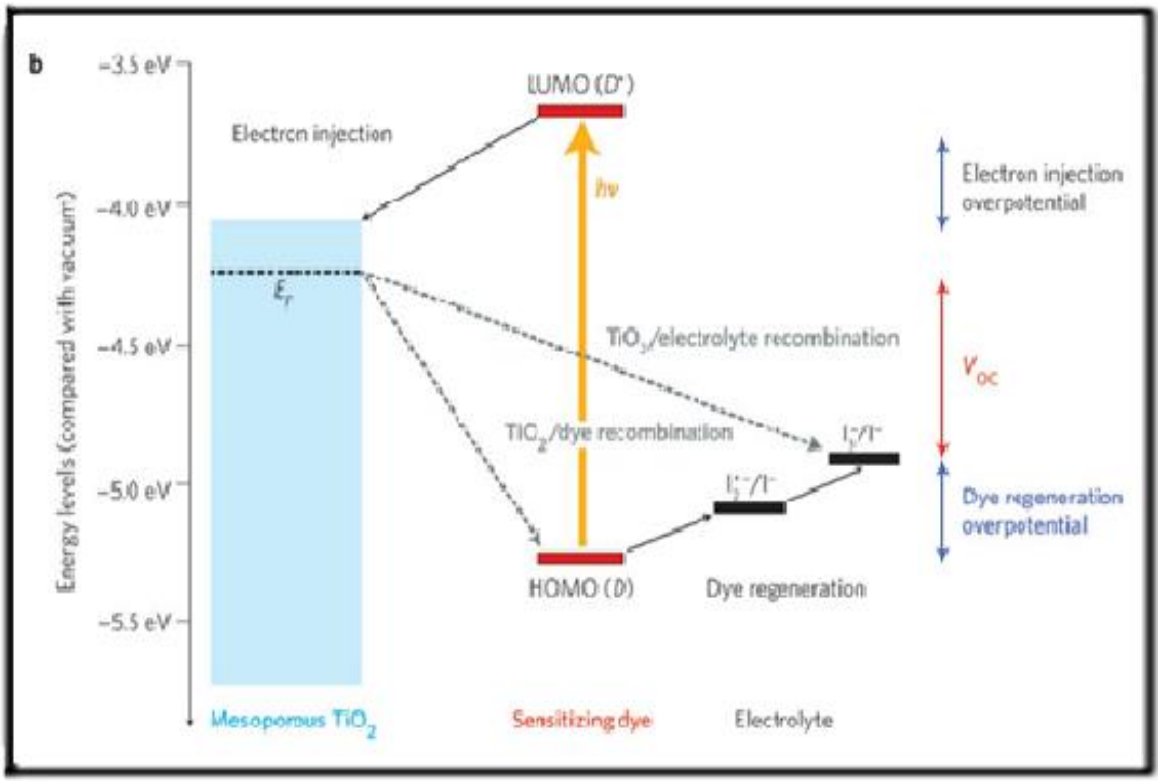

Figure 1.11 (b) Dye-sensitized solar cell operations.[52]

1.9.3.2 Nanorods Sensitized Solar Cell

Nanorods sensitized solar cells are based on ensembles of nanometer size heterointerfaces between two semiconducting nanostructured materials. In this structure nanorods are attached to the large band gap material (TiO_2 or ZnO) through a linker with the bifunctional molecules of the form X-R-Y for linking (X and Y are functional groups, such as carboxylic, thiol *etc*., and the R is an alkyl group) or without a linker molecule, directly attached to the wide band gap material. Finally, a thin layer of liquid electrolyte containing a redox couple or a hole conductor (such as a hole conducting polymer) is sandwiched between this photo electrode and a counter electrode.[65] The device configuration depicted in Figure 1.13 separates the positive and negative photogenerated carriers into different regions of the solar cell using following mechanism: after incident photons are absorbed by the nanorods, photo excited electron-hole pairs are confined within the nanocrystal. If they are not separated quickly, they will simply recombine.

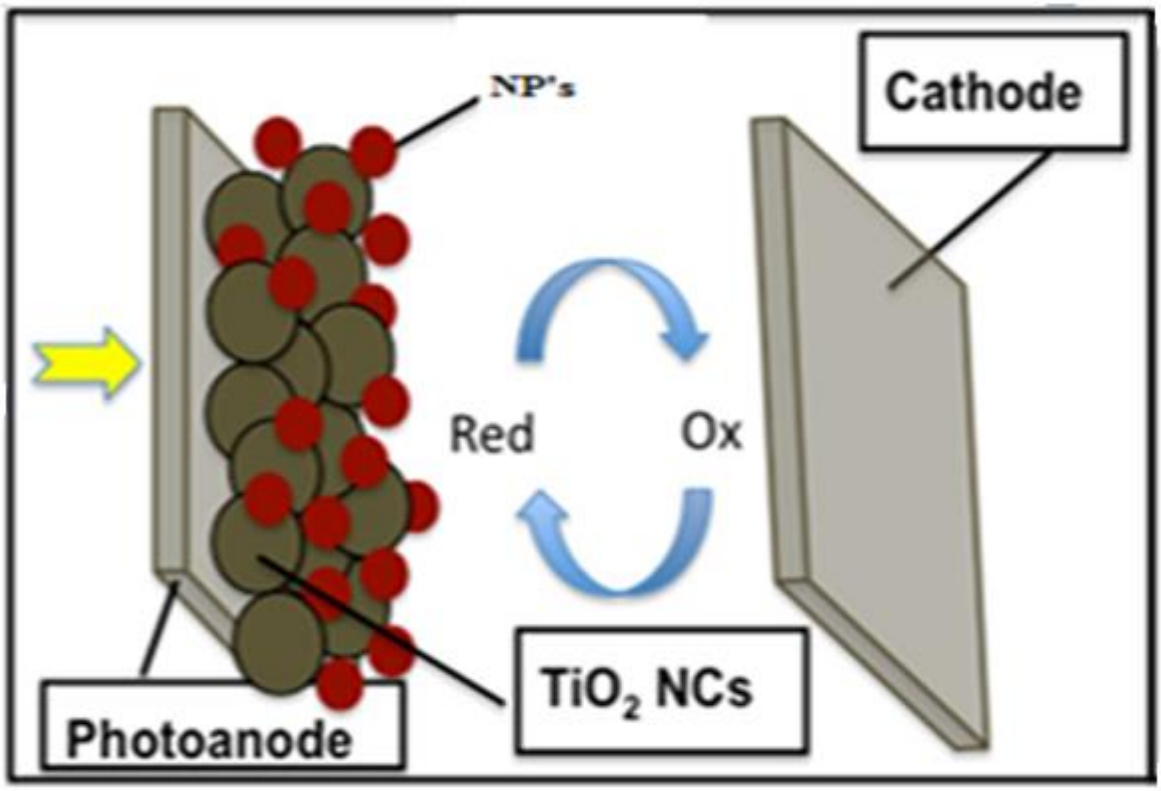

Figure 1.12 Structure of Nanorods-sensitized solar cell. [10]

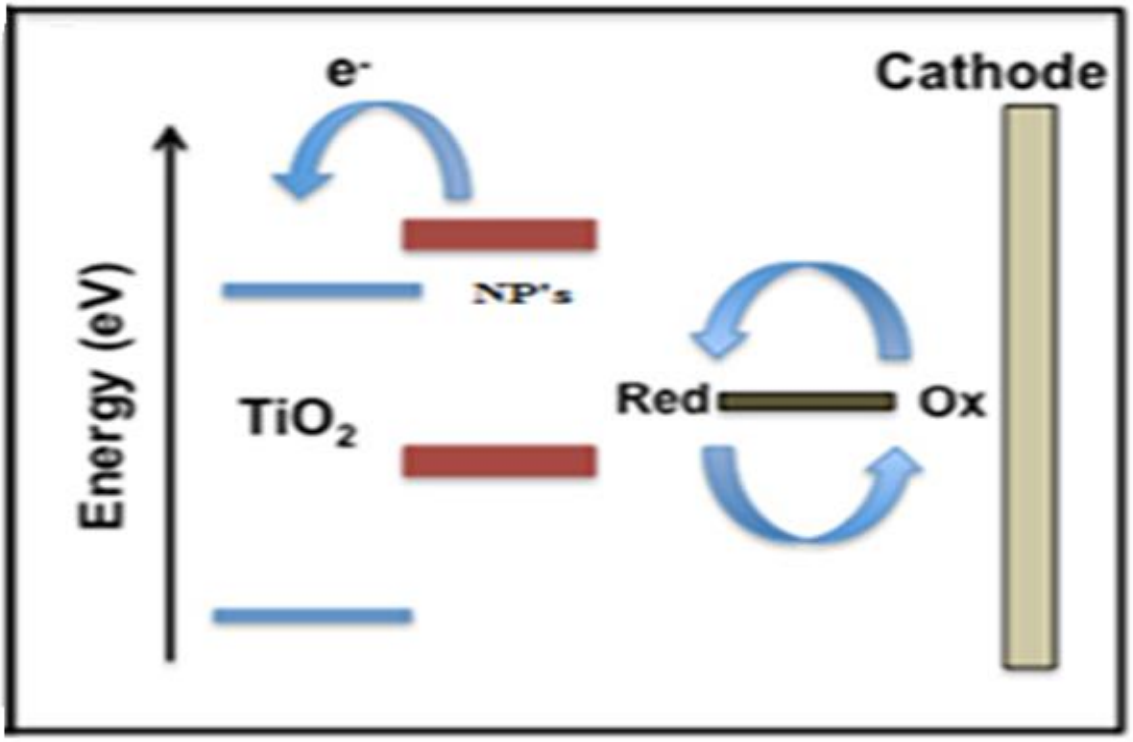

Figure 1.13 Energy level diagram of Nanorods-sensitized solar cell.[10]

After the electron is injected into the metal oxide, the positively charged QD can be neutralized either by hole injection into a hole conductor or through an electrochemical reaction with a redox couple in an electrolyte.[66] The most common deposition techniques in QDSSC are the chemical bath deposition (CBD) and successive ionic adsorption and reaction (SILAR) process in which quantum dots attach directly to wide band gap material. Chemical bath deposition method is one of the inexpensive methods to deposit thin films and nanomaterials. The chemical bath deposition technique requires solution containers and substrate mounting devices. The chemical bath deposition yields stable, adherent, uniform, robust films with good reproducibility by a relatively simple process.[67] The growth of the thin films strongly depends on growth conditions, such as duration of deposition, composition and temperature of the solution and chemical nature of substrate. The SILAR process is based on sequentially reactions at the substrate surface. Accordingly a thin film can be grown layer-by-layer and the thickness of the film is determined by counting the deposition reactions. Examples of wider band gap materials are such as TiO_2.[68,69]

SnO_2. and ZnO Various semiconductor structures were tried in QDSSCs, such as alloys of CdSeS and core shells.[70-74] The sensitization of low-surface-area TiO_2 electrodes with the quantum dot layers increases the performance of solar cell.[75]

1.10 Aims and Objectives

By keeping in mind the importance of nanocrystal based solar cells our aim is to develop nanorods synthesized solar cells with greater efficiency (9%). For this purpose synthesis of CuS nanorods is carried out with the help of co - precipitation method. The reasons for the synthesis of CuS nanorods are

- A low band gap semiconductors (1.2-1.7eV)
- High conductivity.
- Transparent conducting oxide used in solar cells.
- It has very wide absorption window

The current-voltage measurements of CuS: α-Alanine 51 mM gave large J_{sc} and F.F as compared to CuS: α-Alanine 1 mM and the corresponding efficiencies (%) are 1.2 and 0.97 respectively

Chapter 2

Experimental

Section

2.1 Experimental Work

The CuS nanorods have synthesized by co-precipitation method. For the synthesis of CuS nanorods the necessary compounds and chemicals are given in the table along with their chemical formula, chemical name, purity and molecular masses.

2.1.1 Required Chemicals

The chemicals required for the synthesis of CuS nanorods are given in the table 2.1

Table 2.1 List of chemicals used for the synthesis of CuS nanorods.

Sr.No.	**Compound**	**Chemical Formula**	**Molar Mass (g/mol)**	**Purity (%)**	**Suppliers**
1	α-Alanine	$C_3H_7NO_2$	89.056	99	Sigma Aldrich
2	Copper Acetate Monohydrate	$Cu(CH_3COO)_2.H_2O$	199.65	99.5	Sigma Aldrich
3	Thiourea	$(NH_2)_2CS$	76.12	98.5	Sigma Aldrich
4	Sodium Hydroxide	NaOH	40.008	95	Sigma Aldrich
5	Ammonium Hydroxide	NH_4OH	35.04	97	Sigma Aldrich
6	Methanol	CH_3OH	42.032	99	Sigma Aldrich
7	Deionized Water	H_2O	18.016		Chem. Lab

2.2 Synthesis

2.2.1 Synthesis of CuS Nanorods by Co-precipitation Method

Synthesis of CuS nanorods is carried out with the help of co - precipitation method. First of all a mixture of water and methanol 30 mL and 20 mL, respectively was taken in the three-neck flock. By continuous stirring 600 rev / min at 40 °C, different concentration of α-Alanine was added into the mixture. At the same temperature with continuous stirring 0.5 g of copper acetate mono- hydrated was added into the above mixture. After 10 minutes of absolute dissolution 0.5 g of thiourea was taken and dissolved in 10 mL of distilled water separately. This 10 mL solution of thiourea was added into above reaction mixture. For maintaining the pH value 10, we used 5 mM solution of sodium hydroxide drop wise. After maintaining the pH value, the reaction was continued with stirring under argon gas at 40 °C for 50 minutes. At 150 °C with continuous stirring the reaction was carry on for 5 hours after which blackish precipitate of CuS nanorods had obtained, that was our required product. Then stop the reaction and the solution was allowed for 2 hours at the room temperature for cool down. On cooling we got blackish precipitate by the centrifugation process. These precipitates were dried over night at room temperature. At different temperature with the same procedure CuS nanorods can be synthesized.

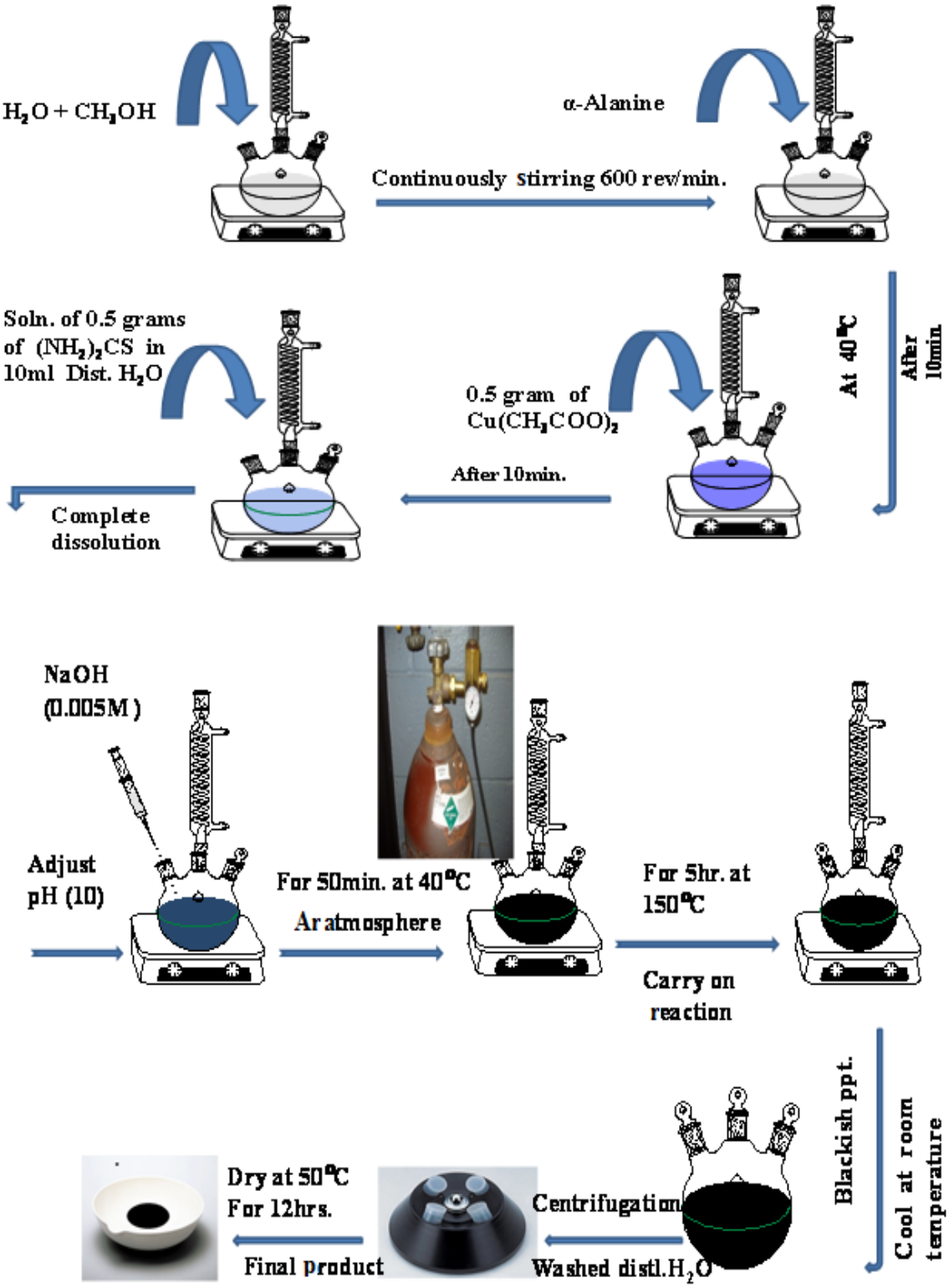

Figure 2.1 Scheme for synthesis of CuS nanorods.

2.3 Solar Cell Fabrication

First of all we prepared CuS nanorods with the help of co- precipitation method by using the α-Alanine as capping agent. We obtained two same sizes (1×3 cm) indium tin oxides (ITO) glasses, washed with acetone, methanol and distl. water to remove the impurity. After this ITO glasses were dry at the room temperature. With the help of multimeter we tested the conducting side of each ITO. On the conducting side place tape along the long and short side of glass plate to overlap 1 mm and 4 to 5 mm respectively. On the conducting side put two drops of TiO_2 and spread it over the plate surface which must be so homogeneous layer. Before all of this there must be coating of tin oxide on one side of plate. On drying overnight titanium dioxide on the plate surface remove the tape. With the help of spin coater the CuS nanorods coating has been done and it was drying overnight at room temperature. The Pt counter electrode is used. The redox couple (iodide triiodide) is used. By solar simulator the Current Voltage measurement of nanorods synthesized solar cell was taken and the efficiency was calculated by Current Voltage measurement.

2.4 Characterization Techniques

2.4.1 X-Ray Diffraction Technique (XRD)

In order to establish grain size, strain state of materials, structural information and phase composition the XRD is one of the elementary and powerful technique. It is also non destructive technique; this benefit makes it advanced for evaluating structure. It explains that angle of incidence might be calculated very simply in the term of path difference among a ray reflected through one plane and that reflected by next plane in lattice. The desiring nanomaterials have been recognized with help of computerized library present in system by comparing the intensities, positions of the peaks, interpretation and quantification of multiple peaks in a sample may be carried out, yet if one phase of the targeted material is amorphous or relative ratio of each phase using XRD technique. Size of nanoparticles also affects to shape of XRD peaks, mostly in narrow peaks symbolizes to bulk sized materials even as broad peaks in fact represents the small sized material. When the crystals of nanoparticles are lesser than 100 nm then the broad diffracted peaks emerges.

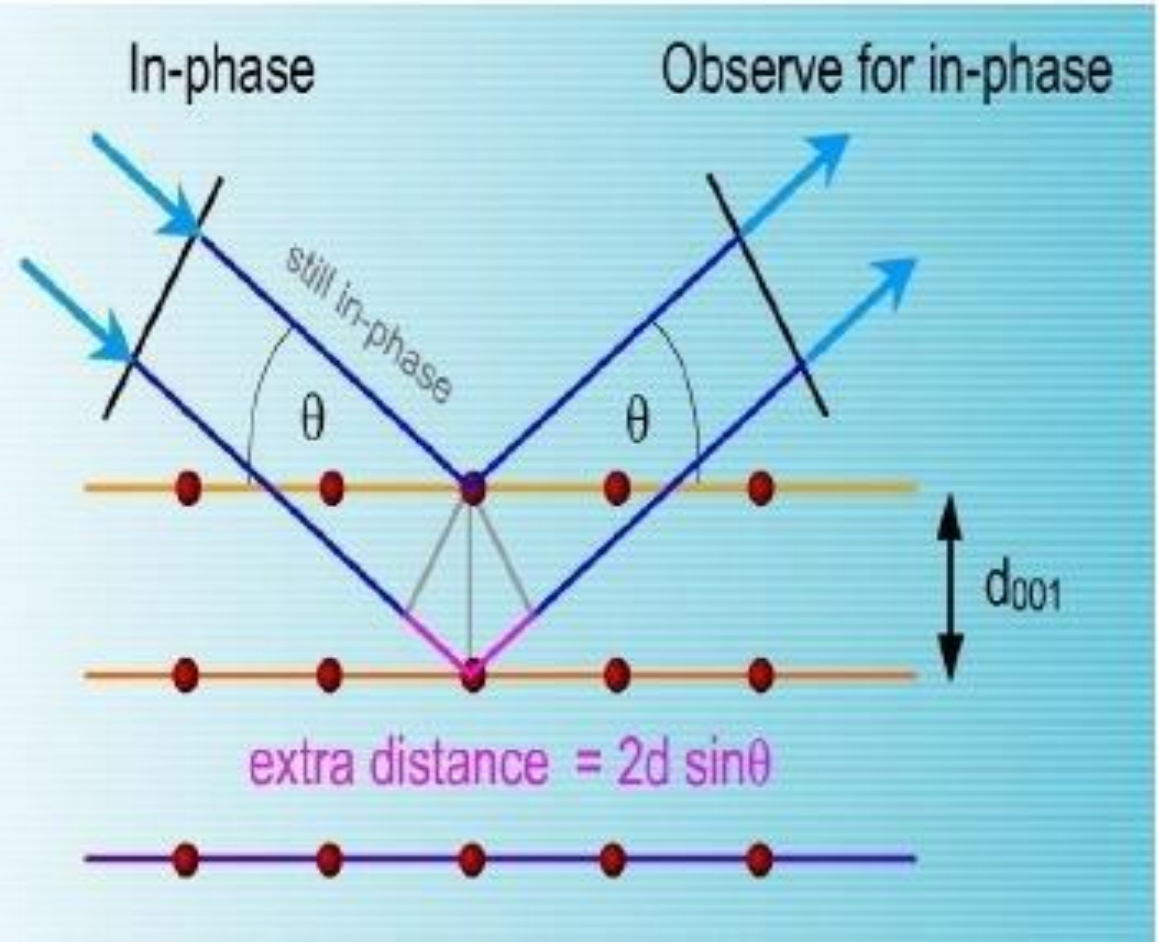

Figure 2.2 Diagram of X-rays diffraction .[76]

2.4.1.2 Principle of X-Ray Diffraction

X-ray diffraction is the currently a common technique for the examine of crystal structure. For crystalline sample the X-ray diffraction is based upon the constructive interference of monochromatic X-rays. The contact of the incident rays and the sample creates constructive interference on satisfying the Bragg's Law ($n\lambda=2d \sin\theta$). Then these diffracted X-rays have been detected, processed and counted. The light which have been scattered from material is studied and the structure information about crystal materials is attained. Every crystalline material has a unique X-rays pattern called as a "fingerprint". Interaction between X-rays and crystalline phase offers a diffraction pattern**.** The alteration of diffraction peaks to the d-spacings permits identification of mineral due to unique set of d-spacings of each mineral. Normally this is attained by contrast of d-spacings with the standard reference patterns. The CuS nanorods material was analyzed by XRD (X'PERT PRO) instrument.

Figure 2.3 X' PERT PRO XRD instrument

2.4.2 Fourier Transform Infrared Spectroscopy (FTIR)

It is used to get the infrared spectrum of the absorption and emission results of solid, liquid or gas. It tells about the functional group present in the sample. The wave number range of the instrument (FTIR Alpha-P) is from wave number 400 to 4000 cm^{-1}**.** The spectrum got from instrument gives the information regarding the vibrational modes of sample in IR region of the electromagnetic radiations. The interferogram basically measures in wavelength and fourier transform converts it in the wave number domain that is why it is termed as fourier transform infrared spectroscopy. The IR radiations are incidents on the sample some of frequencies are absorbed while rests of frequencies are transmitted. Absorbed frequencies match with vibrational frequencies of the analyzed species that is why it also called vibrational spectroscopy.

2.4.2.1 Advantages of FTIR Spectrometer

FTIR spectrometers belong to the third generation infrared spectrometer. FTIR spectrometers have many well-known advantages:

- There is significantly high signal to noise ratio of the spectra as compare to earlier generation infrared spectrometers
- High accuracy of wave number is present. The error range is within the ± 0.01 $cm^{1.}$
- The scanning time of all the frequencies is very short approximately equal to 1s.

- It has high resolution as compare to previous infrared spectrometers.
- It has wide scanning range (1000 ~ 10 cm^{-1}).
- The interference from wandering light is reduced.

2.4.3 Ultraviolet Visible Spectroscopy (UV-Visible)

UV-Visible spectroscopy is known as electronic spectroscopy. UV-Visible spectroscopy is the major technique for the determination of the optical properties of nanoparticles. The incorporation of the ultraviolet or visible radiation by a molecule guides transition among the electronic energy levels of the molecule. The wavelength range for the ultraviolet and visible is 190-400 nm and 400-800 nm respectively. UV-Visible (Schimadzu 1601) spectrophotometer was used to characterize dispersed, transparent and diluted solutions.

2.4.3.1 Principle of Ultraviolet-Visible Spectroscopy

The larger number of molecules will be absorbed greater extent of light as result higher the peak intensity in the absorption spectra. If few molecules will absorb radiation then the overall absorption of energy is small and lower the peak intensity is observed in the absorption spectra. This creates the basis of Beer-Lambert Law which explains the fraction of incident radiation absorbed has proportional relation to the number of absorbing molecules in its pathway. When the radiations of specific wavelength and frequency pass through a solution then the quantity of light absorbed or transmitted is exponential function of solute concentration and also function of path length of cell through radiations pass.

So

$$\text{Log } I_o / I = \varepsilon\, c\, l \qquad (2)$$

Where

I_o = Intensity of the incident light

I = Intensity of transmitted light

c = Concentration of the solute in mol l^{-1}

l = Path length in cm

ε = Molar extinction coefficient

Molar extinction coefficient is a characteristic constant and is numerically equal to absorbance of a solution of unit molar concentration (c = 1) in a cell of unit length (l = 1) and its unit is liters $mol.^{-1}$ cm^{-1}. The ratio I / I_o is known as transmittance which is

indicated by ‘ T ’ and the logarithm of inverse ratio I_o / I is well-known as the absorbance which is indicated by ‘ A ’.

Thus

$$- \text{Log } I / I_o = - \log T = \varepsilon c l$$

$$\text{Log } I_o / I = A = \varepsilon c l$$

Or

$$A = \varepsilon c l \quad (3)$$

2.4.4 Photoluminescence Spectroscopy (PL)

Photoluminescence spectroscopy is utilized to measure fluorescence of molecules after excitation. It is planned to investigate the energy states through the excitation of the electrons in a singlet ground state to an excited singlet state using the absorption of radiation and the consequent emission of absorbed energy in the form of photon. In excited state, the electron may experience radiative or non-radiative relaxation routes such as releasing energy to the vibrational levels of the solvent or decay using inter-system crossing to the triplet state and the phosphorescence. The Phosphorescence is the longer existed method than fluorescence, due to inter-system crossing among a singlet and triplet state being properly forbidden. The photoluminescence measurements were determined with fluorescence spectrophotometer (Flau Time 300). A characteristic spectrophotometer requires a high energy source such as a xenon lamp or a laser for the activation. Laser has an extremely narrow emission wavelength and not need an excitation monochromator, but excitation wavelength cannot be altered exclusive of changing the laser. The xenon source is a constant wave source with the near regular emission intensity having 300 - 800 nm wavelength range.

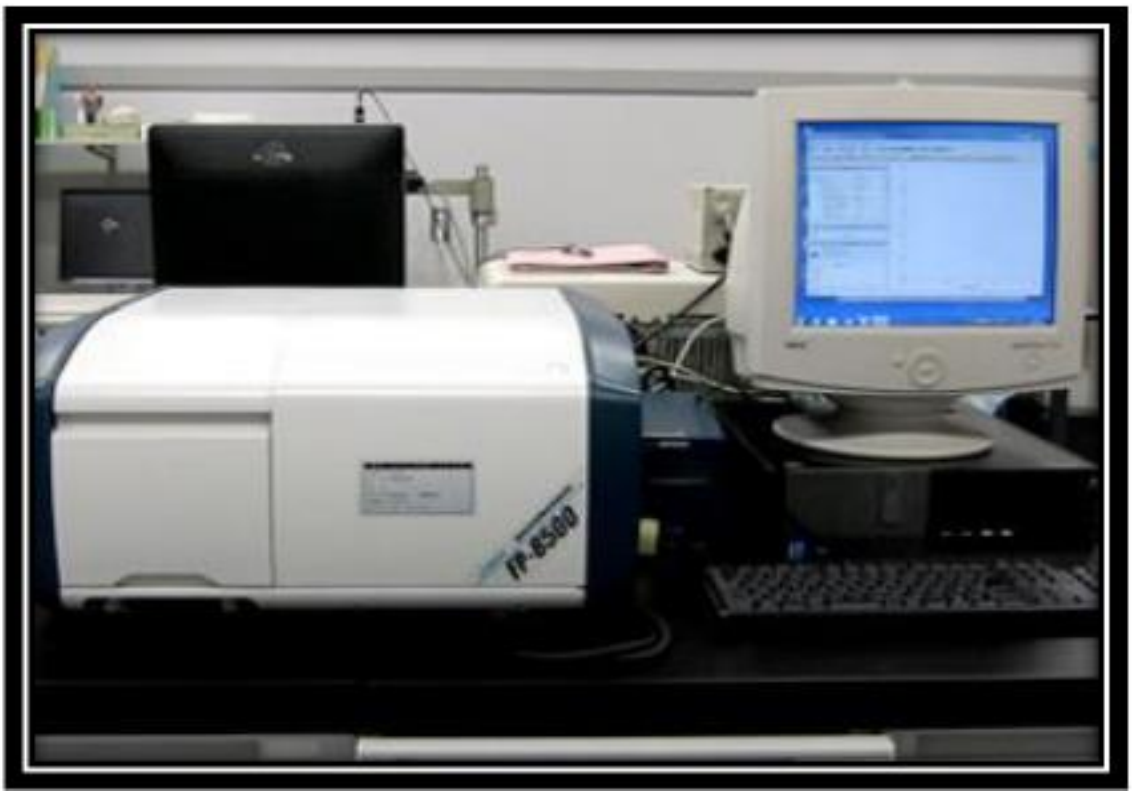

Figure 2.4 Fluorescence Spectrometer

2.4.4.1 Principle of Photoluminescence Spectroscopy (PL)

Photoluminescence (PL) spectroscopy is the major technique for the determination of the optical properties of nanoparticles. It is the more sensitive than absorption measurements. In photoluminescence spectroscopy mostly emission spectrum is studied and also it deals with the electronic and vibrational state. In which the molecule are excited, through the absorption of photon from its ground electronic state to one of the various vibrational states in the excited electronic state. Collision of excited molecule with other molecules cause the excited molecule to lose vibrational energy until it reaches the lowest vibrational state of the excited electronic state.

2.4.5 Scanning Electron Microscopy (SEM)

It is a sort of electron microscope that creates images of the sample by scanning it with a focused beam of electrons. The electrons interrelate with atoms in the sample and producing a variety of signals that have information about the surface of sample and its composition. The electron beam is commonly scanned in a raster scan pattern and the beam's location is merged with the detected signal to create an image. Scanning electron microscope is a type of (FESEM MIRA 3 XMU coupled with EDX) electron microscope. SEM can get resolution better than 1 nanometer. SEM primarily shows the three-

dimensional structure of the material's surface. Samples in the dry form were prepared for SEM analysis. But aggregates formation occur during drying particles due to large surface tension which making it difficult to visualize the individual nanostructured material. To overcome this problem we dispersed the nanoparticles of CuS in the fast drying solvent like ethanol or acetone because it does not react chemically with the CuS nanoparticles. The most ordinary SEM form is detection of secondary electrons released by atoms which is excited by the electron beam. On sample scanning the secondary electrons are collected that are released using an unusual detector and an image showing the topography of the surface is created.

Figure 2.5 Scanning electron microscope

2.4.5.1 Principle of Scanning Electron Microscopy (SEM)

The signals upshots from the interaction of electrons beam with the atoms at a variety of depths within the sample. In most general detection mode, the secondary electron imaging or secondary electrons are released through extremely close to the sample surface. The SEM utilizes electron beam as an alternative of the light beam towards sample under examination. When interaction of the electrons with atoms in sample is occur, it creates a variety of signals which have information about sample topography. Signals emitted by beam of the electrons after interaction with the atoms

contained X-rays and three types of electrons these are named as primary back scattered, secondary and auger electrons. X-rays will be utilized to identify its composition and plenty of the elements in sample. The Scanning Electron Microscopy creates high resolution pictures of the sample surface, illuminating the detail less than the 1 nm in dimension. In present work, the SEM images were collected by secondary electron detector.

2.5 Solar Simulator

Solar simulator (Keithley-2420 source meter with xenon lamp type B simulator) used to measure the current voltage response of nanorods sensitized solar cell. A solar simulator is also called artificial sun. This device provided us illumination which is approximately equal to natural sunlight.The purpose of the solar simulator is to offer a well regulated indoor test facility under laboratory conditions. Solar simulator is mostly used for the testing of solar cells. But it is also used for analysis of sun screen, plastics and other materials and devices. In solar cells analysis we measured open circuit voltage (V_{oc}), short circuit current (J_{sc}), fill factor (FF), maximum power point (P_{mp}) and an efficiency of solar cell.

Chapter 3

Results
&
Discussion

3.1 Characterizations of Synthesized CuS Nanorods

3.1.1 SEM Analysis of CuS Nanorods Using 1 mM of α-Alanine

The SEM analysis is normally used to find out the morphology of the nanomaterials. This technique gives information about surface roughness, porosity, intermetallic distribution, material homogeneity, and particle size. The SEM analysis corroborated that the CuS nanoparticles were effectively synthesized. Firstly the SEM image was taken at magnification power of 5.00 kx with 10 μm scale which indicate the formation of CuS nanorods which are agglomerated with irregular pattern as shown in the figure 3.1 (a). This aggregates formation occur during drying of particles due to large surface tension which making it difficult to visualize the individual nanostructured material. The size of CuS nanorods cannot be clearly seen at this magnification power so for further clearance we increased the magnification power up to 50 kx with 1μm. As indicated in figure 3.2 (b) the synthesized CuS material is appeared in the form of nanorods with different length and width. In thesis SEM image it is clear that our synthesized CuS nanorods are homogeneous throughout. The magnification power equipped with 100 kx and 500 nm scale (figure 3.1 (c)) confirmed that the grown nanorods have approximately 100 nm length and 30 nm width.

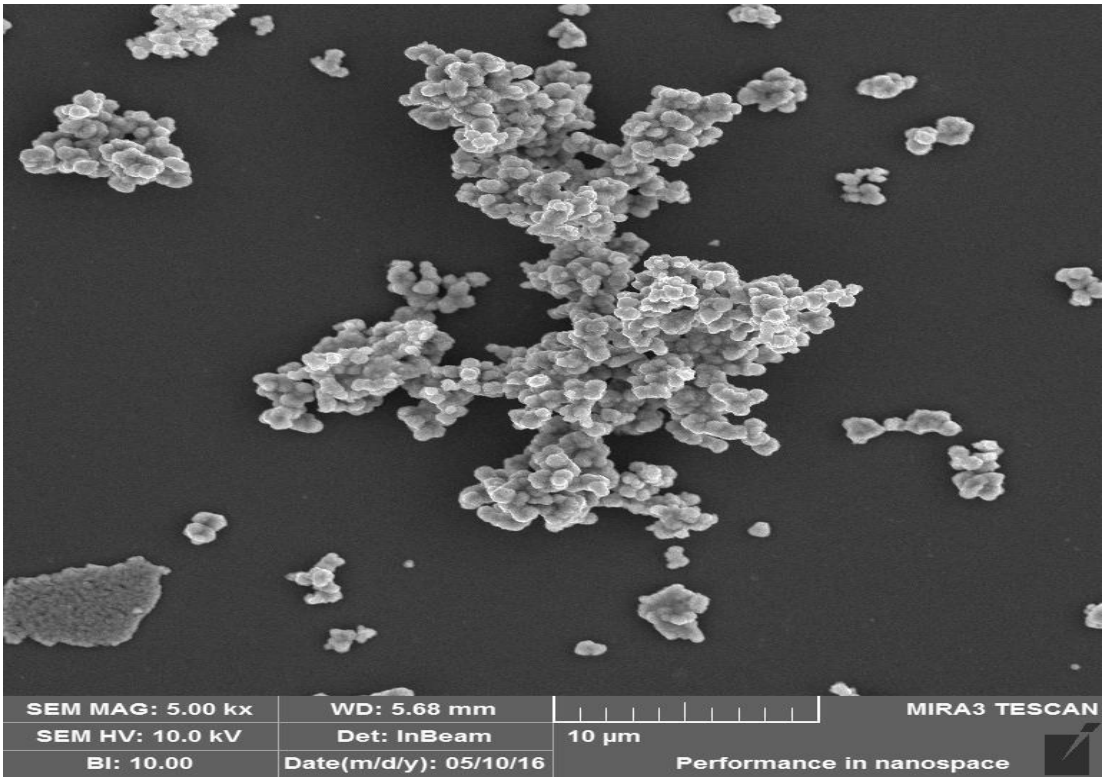

Figure3.1 (a) SEM image of CuS nanorods at 5 kx magnification power.

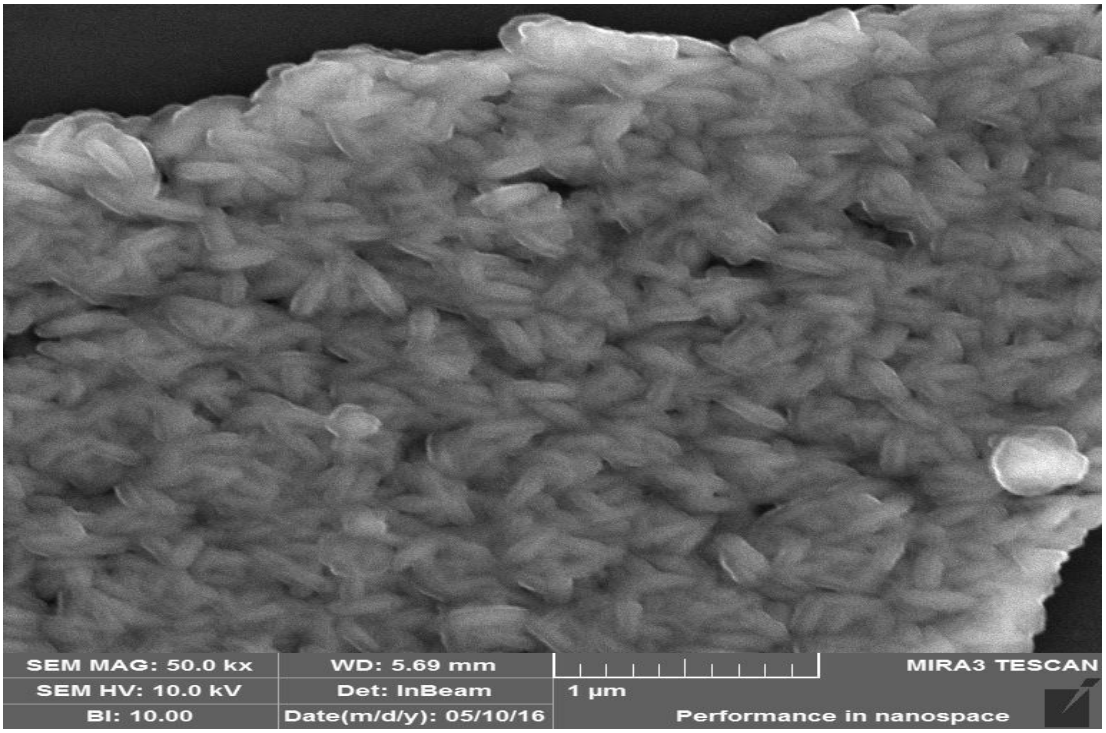

Figure 3.1 (b) SEM image of CuS nanorods at 50 kx magnification power.

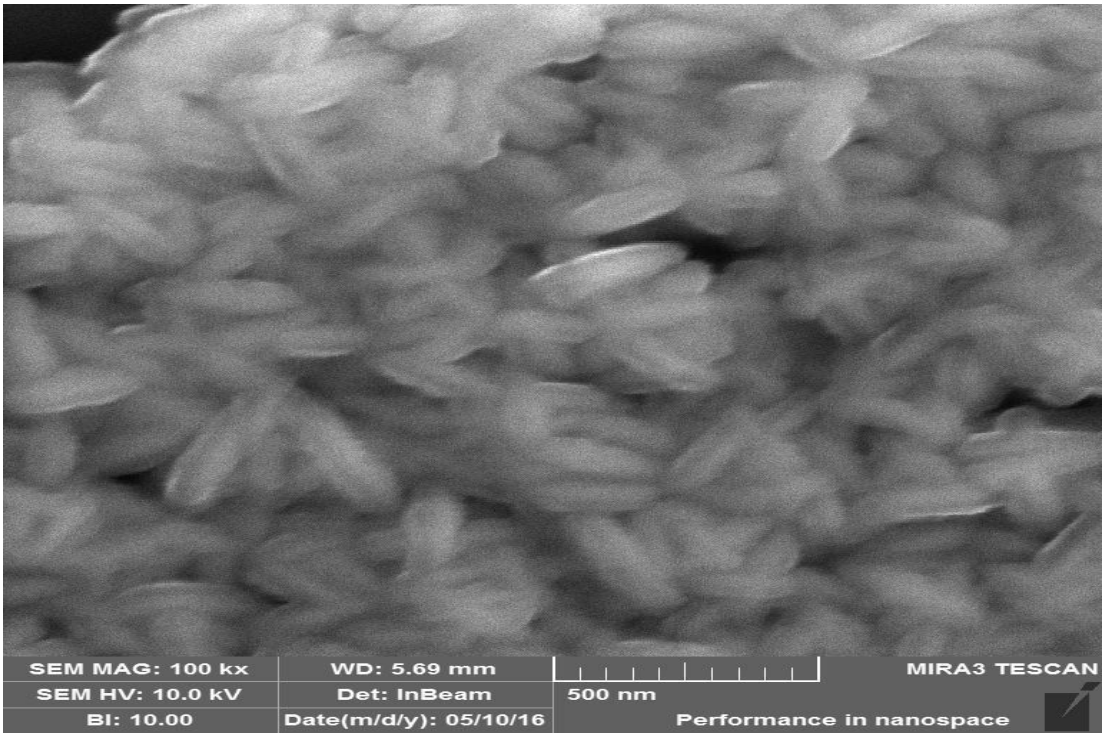

Figure 3.1 (c) SEM image of CuS nanorods at 100 kx magnification power.

3.1.2 EDX Analysis of CuS Nanorods Using 1 mM of α-Alanine

The EDX images of CuS nanorods are shown in figure 3.2. It confirmed the presence of copper and sulphur in synthesized CuS Nanorods.

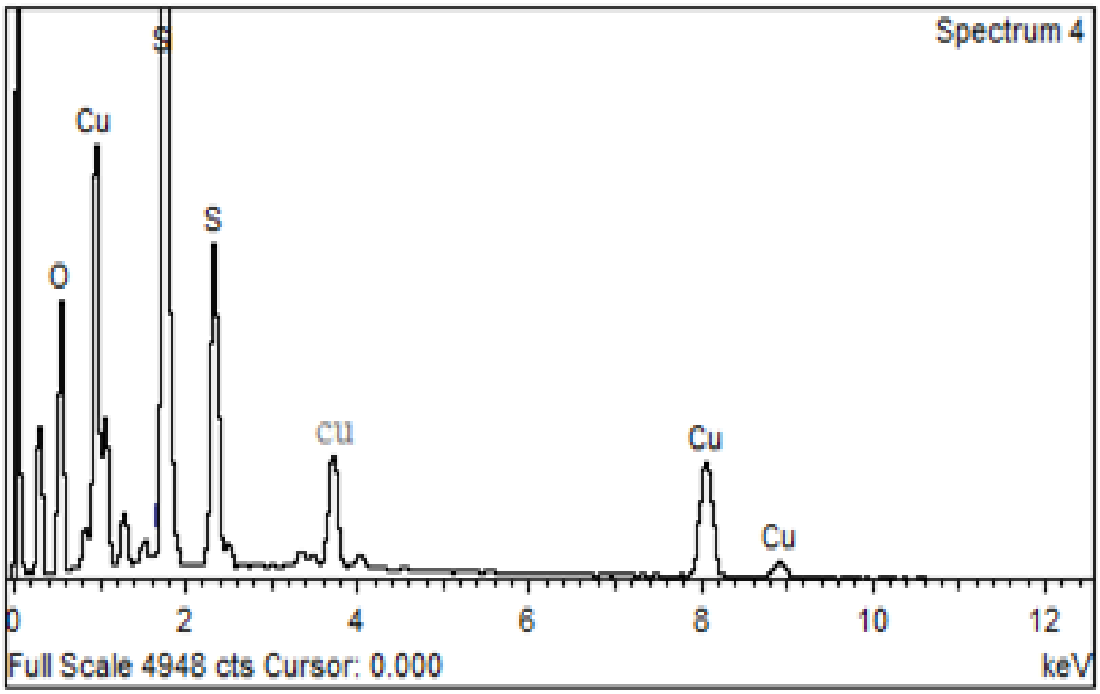

Figure 3.2 EDX image of CuS nanorods

The elemental analysis of CuS nanorods in the atomic % and the weight % are shown in the table 3.1.

Table 3.1. EDX analysis of CuS nanorods.

Elements	**Weight %**	**Atomic %**
Cu	56.45	62.23
S	40.25	36.02
O	3.3	1.75
Total	100%	100%

In elemental analysis of CuS nanorods the oxygen (O) element may be present due to the capping agent α-Alanine and sulfur (S) also comes from the anionic precursor which is thiourea. The greater presence of cupper (Cu) is due to the cationic precursor (cupper acetate) and the presence of the Cu and S tells us about the formation of CuS nanorods. The impurity is due to the capping agent and some due to the unreacted reactants. This impurity can be minimized by more washing and usage of more pure chemicals.

3.1.3 FTIR Spectrum of CuS Nanorods Using 1 mM of α-Alanine

FTIR analysis has been done in order to examine whether the capping process of CuS nanorods by α-Alanine was successful or not. This type of spectroscopy used extensively to examine the interaction of nanoparticles with the functional groups of the α-Alanine. In order to assess the interaction of CuS nanoparticles with α-Alanine has been distinguished by FTIR in the given figure 3.3. The signal at wave number 609 cm^{-1} demonstrates the existence of CuS. Two signals having wave number 3550 cm^{-1} and 3000 cm^{-1} demonstrates the existence of $–NH_2$ that may have been come from α-Alanine and bulky group respectively. The C=S peak appeared at the wave number 1501 cm^{-1} that is due to the contribution of thiourea as precursor. The –OH peak appears at 3736 cm^{-1} that may come from water or NaOH.

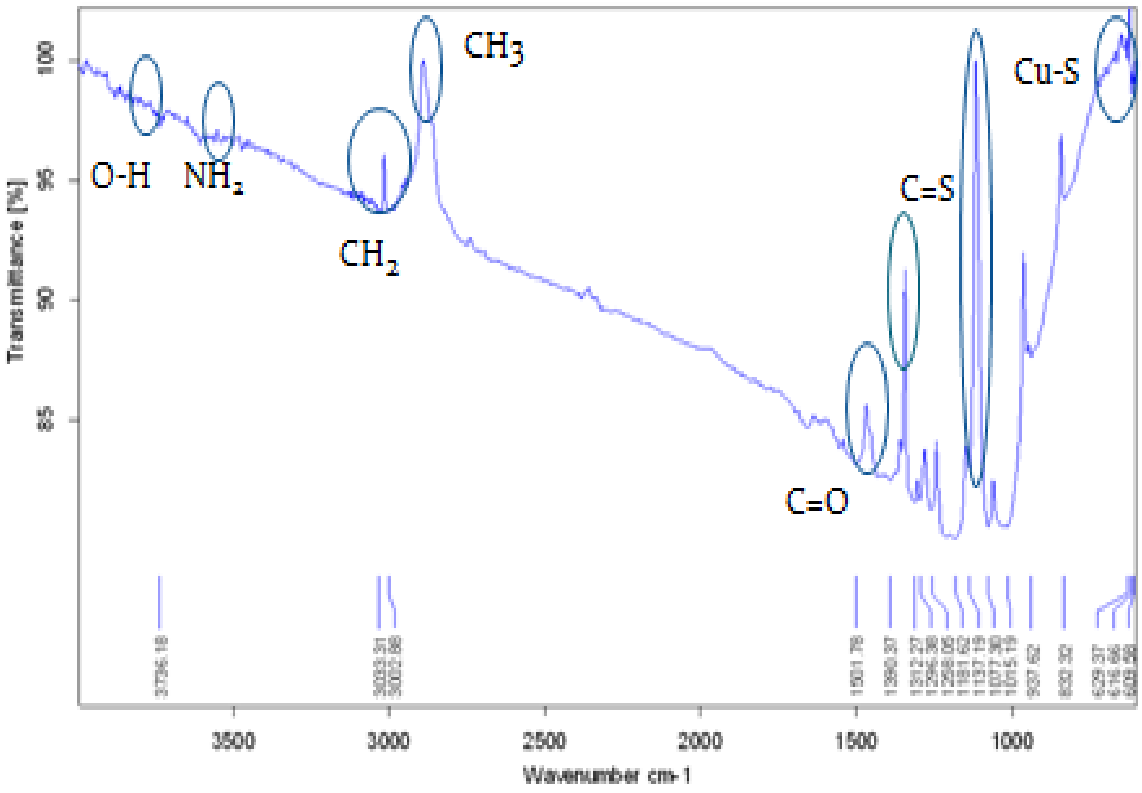

Figure 3.3 FTIR spectrum of CuS Nanorods using 1 mM of α-Alanine.

3.1.4 XRD Pattern of CuS Nanorods Using 1 mM of α-Alanine

In order to calculate the grain size, structural information, composition of phase and strain state of materials X-Ray Diffraction is considered the best powerful technique. Moreover broadening of XRD peaks confirm small size of CuS. XRD patterns peaks of capped CuS nanorods have attained at the 2θ scale, 23.0^0, 29.2^0, 31.5^0, 33.4^0, 49^0, 59^0 corresponds to (004), (101), (102), (103), (110), (116) planes of standard hexagonal structure as shown in figure 3.3. All these peaks obviously indicate the presence of hexagonal structure. All XRD peaks of CuS NPs considerably attained intense and broad which obviously point out presence of metallic copper at nanometre scale. From this XRD pattern the value of full width half maxima (FWHM) is equal to 0.29^o. The size of CuS nanorods in this case is 29 nm.

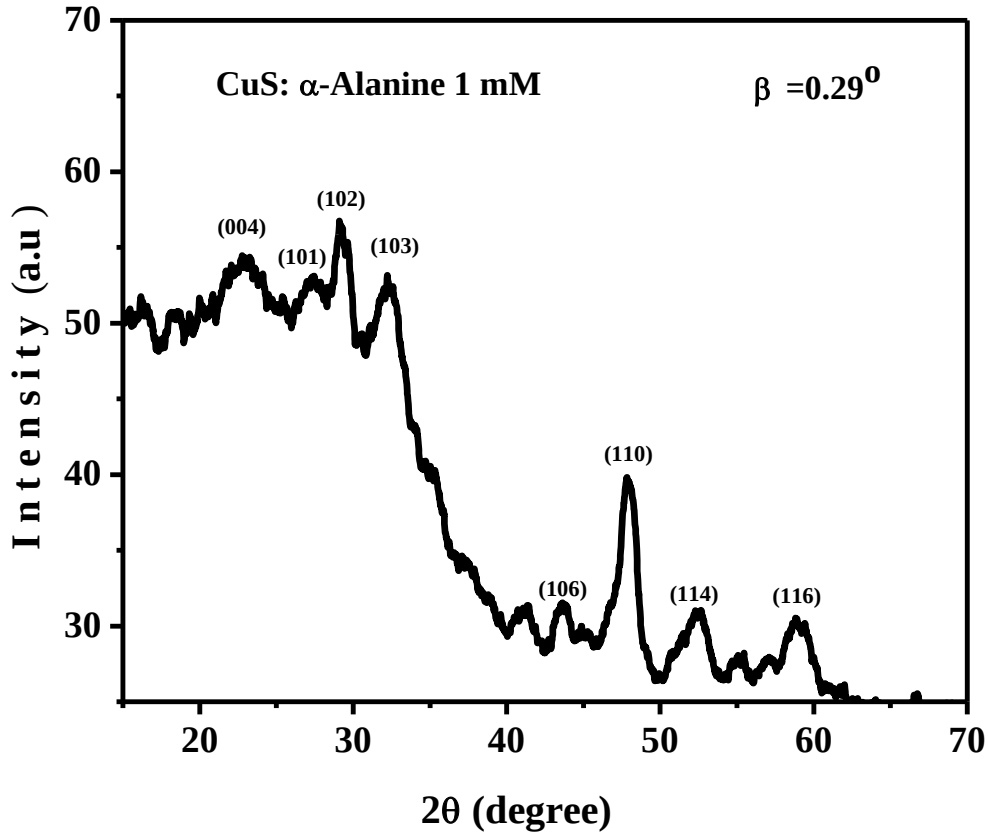

Figure 3.4 XRD Pattern of CuS Nanorods using 1 mM of α-Alanine.

3.1.4.1 Comparison of XRD Patterns

First of all different sample were synthesized by using the different concentration of capping agent (α-Alanine) but having the same concentration of both precursors. The method for the formation of different sample is same as for the synthesized CuS nanorods using 1 mM of α-Alanine as shown in the scheme figure 2.1**.**

The XRD Characterization of Synthesized CuS nanorods using 11 mM of α-Alanine shows that the peaks position is approximately same such as in the case of 1 mM of α-Alanine. The more intense peaks are observed in the case of 11 mM of α-Alanine and also the more broad peaks are appeared by increasing the concentration of capping agent. From this XRD pattern the value of full width half maxima (FWHM) is equal to 0.47^{o} and crystalline size of CuS nanorods calculated by Scherer's formula in this case is 23 nm. This increase in full width half maxima value indicates the decrease in size of synthesized material. The XRD patterns peaks of capped CuS nanorods were attained at the 2θ scale, 23^{0}, 29.2^{0}, 31.5^{0}, 33.4^{0}, 49^{0}, 53^{0}, 59^{0} corresponds to (004), (101), (102), (103), (110),

(114), (116) planes of standard hexagonal structure. All these peaks obviously indicate the presence of hexagonal structure. All XRD peaks of CuS nanorods considerably attained intense and broad which obviously point out presence of metallic copper at nanometre scale.

The synthesized CuS nanorods by using 21 mM of α-Alanine shows that the broader and intense peak at the 59^0 as compared to previous cases which is the indication of increase in full width half maxima value. From this XRD pattern the value of full width half maximum is equal to 0.76^0. This Broadening of XRD peaks confirm small size of CuS nanorods. In this XRD pattern all the peaks of CuS nanorods considerably attained intense and broad which obviously point out presence of metallic copper at nanometre scale. In this sample the calculated crystalline size is equal to 16 nm. Similarly by using 21 mM of α-Alanine all the peaks obviously indicate the presence of hexagonal structure.

All the peaks in the XRD characterization of Synthesized CuS nanorods using 31 mM α-Alanine indicate more intensity. By further increasing the concentration of α-Alanine more broadening of peaks is occurred. The XRD pattern peaks of capped CuS nanorods synthesized by using 31 mM of α-Alanine were attained at the 2θ scale, 27^0, 29.2^0, 31.5^0, 33.4^0, 37^0, 49^0, 52.5^0, 59^0 corresponds to (101), (101), (102), (103), (105), (110), (114), (116) planes of standard hexagonal structure as shown in figure 3.5. This XRD pattern of Synthesized CuS nanorods using 31 mM of α-Alanine shows that the peaks position is approximately same such as in the case of 1 mM of α-Alanine. From this XRD pattern the value of full width half maximum is equal to 0.94^0 and calculated crystalline size by Scherer's formula is equal to 10 nm. This decrease in size is due to more increase value of full width half maxima, more intense and broadening of peaks by increasing the concentration of capping agent. Both the peaks appeared at 33.4^0 and 59^0 having more intensity and broadness as compared to the CuS nanorods synthesized by using the 1 mM of α-Alanine.

In the next one sample of CuS nanorods synthesized by using the 41 mM of α-Alanine gives the four XRD more broad peaks at 29.2^0, 31.5^0, 49^0 and 59^0 as compared to sample formed by 1 mM of α-Alanine. In this sample all XRD peaks of CuS nanorods considerably attained intense and broad. This broadening of XRD peaks shows the further reduction in size of nanoparticles. The full width half maximum is equal to 1.15^0. The crystalline size calculated by Scherer's formula is equal to 8 nm. All the peaks in this XRD pattern were attained at the 2θ scale, 23.0^0, 29.2^0, 31.5^0, 33.4^0, 44^0, 49^0, 52^0, 59^0

corresponds to (004), (101), (102), (103), (106), (110), (114), (116) planes of standard hexagonal structure. Similarly for all previous samples this sample also has peaks which obviously indicate the presence of hexagonal structure. Approximately in the entire XRD sample the peaks position occurred at the same 2θ value which indicates that in all the cases same required product is formed just the change occurs in the intensity and broadening of the peaks. By this changing the value of full width half maxima is also changed. Mostly by increasing the concentration of capping agent (α-Alanine) the value of full width half maxima is also increased in all cases which indicate the decrease in the size of nanomaterials.

The XRD characterization of synthesized CuS nanoparticle by using 51 mM of α-Alanine shows that all XRD peaks of CuS nanorods considerably attained intense and broad due to this broadening of XRD peaks confirm small size. The XRD pattern peaks of capped CuS nanoparticles were attained at the 2θ scale, 29.2^0, 31.5^0, 39^0, 44^0, 49^0, 53^0, 59^0 corresponds to (102), (103), (105), (106), (110), (114), (116) planes of standard hexagonal structure. All these peaks also obviously indicate the presence of hexagonal structure. From this XRD pattern the value of full width half maxima (FWHM) is equal to 1.152^0 and crystalline size calculated by Sharer's equation is equal to 8 nm.

The Comparison of all XRD spectra are given in the below figure 3.5. XRD patterns suggested that CuS nanorods were grown in hexagonal crystal structure and by increasing the concentration of capping agent (α-Alanine) the β value (β = FWHM) is also increased . The increase in the β value gives the smaller size of CuS nanoparticles. XRD patterns proposed that by increasing the concentration of α-Alanine, the reduction in size is observed in the CuS nanoparticles.

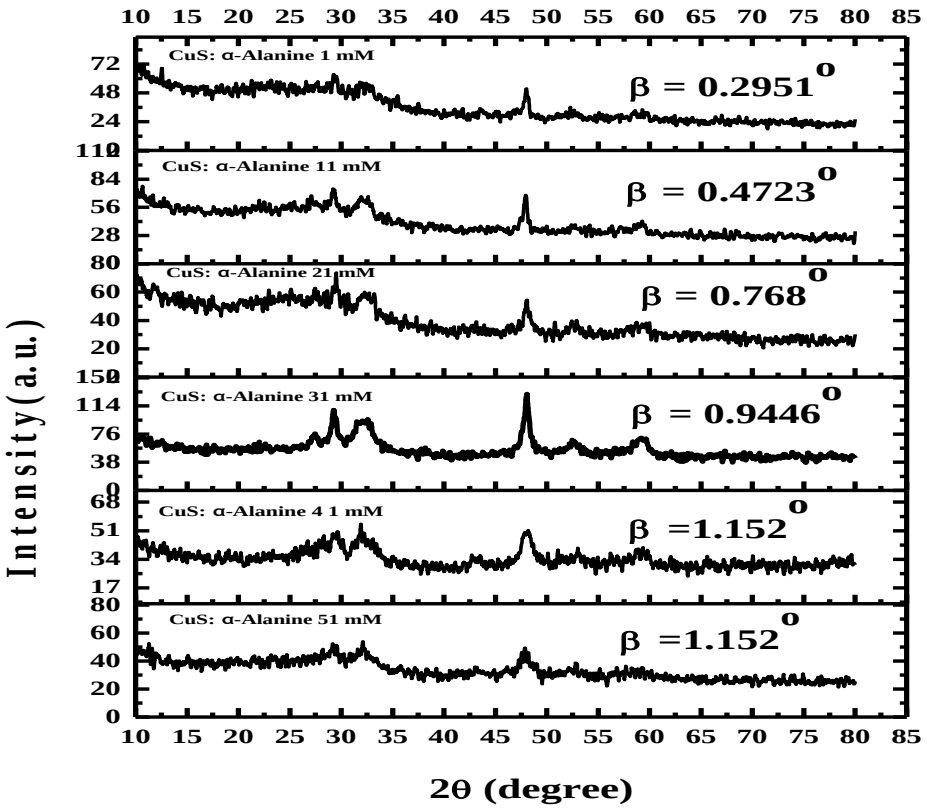

Figure 3.5 XRD Spectra of CuS Nanorods using different concentration of α-Alanine

The crystalline size from XRD pattern was calculated by using the Debye Scherer's formula:

$$d = \frac{k\lambda}{\beta \cos\theta}$$

Where

Θ = Bragg's angle

λ = Incident X-ray wavelength (Radiation source Cukα = 1.5404 Å)

β = FWHM (Full width at the half maximum)

d = Crystallite size

Table 3.2 Crystallite Size of CuS Nanorods from XRD Patterns.

Sr.No.	Sample name	FWHM (degree)	2θ (degree)	Size (nm)
1	CuS: α-Alanine 1 mM	0.29	47.88	29
2	CuS: α-Alanine 11 mM	0.47	47.98	23
3	CuS: α-Alanine 21 mM	0.76	48.05	16
4	CuS: α-Alanine 31 mM	0.94	48.05	10
5	CuS: α-Alanine 4 1 mM	1.15	47.93	8
6	CuS: α-Alanine 51 mM	1.152	47.99	8

The calculated average crystallite size of all the samples with the different concentration of α-Alanine is 15.6 nm.

3.1.5 UV-Visible Spectrum of CuS Nanorods Using 1 mM of α-Alanine

Ultraviolet visible spectroscopy is the major technique for the determination of the optical properties of nanoparticles. UV-visible absorption spectrum of CuS nanorods in the water solvent was measured at the wavelength range of 200-1100 nm which is shown in the figure 3.6. The maximum absorption of smaller band gap CuS nanorods is beyond the 1100 nm. In the visible region an absorption peak is appeared at around 584 nm. This peak has broad absorption which is due to the electronic transition from valence band of CuS to first conduction band. This broadness is due to the various energy surface states which are present among the valence and conduction bands of CuS. Less sharpness of peak at 584 nm showed that there is various surface energy states present among the valence and conduction bands of CuS. Band gap of CuS is small. Due to the very wide absorption window, this is good material for the application in solar cell.

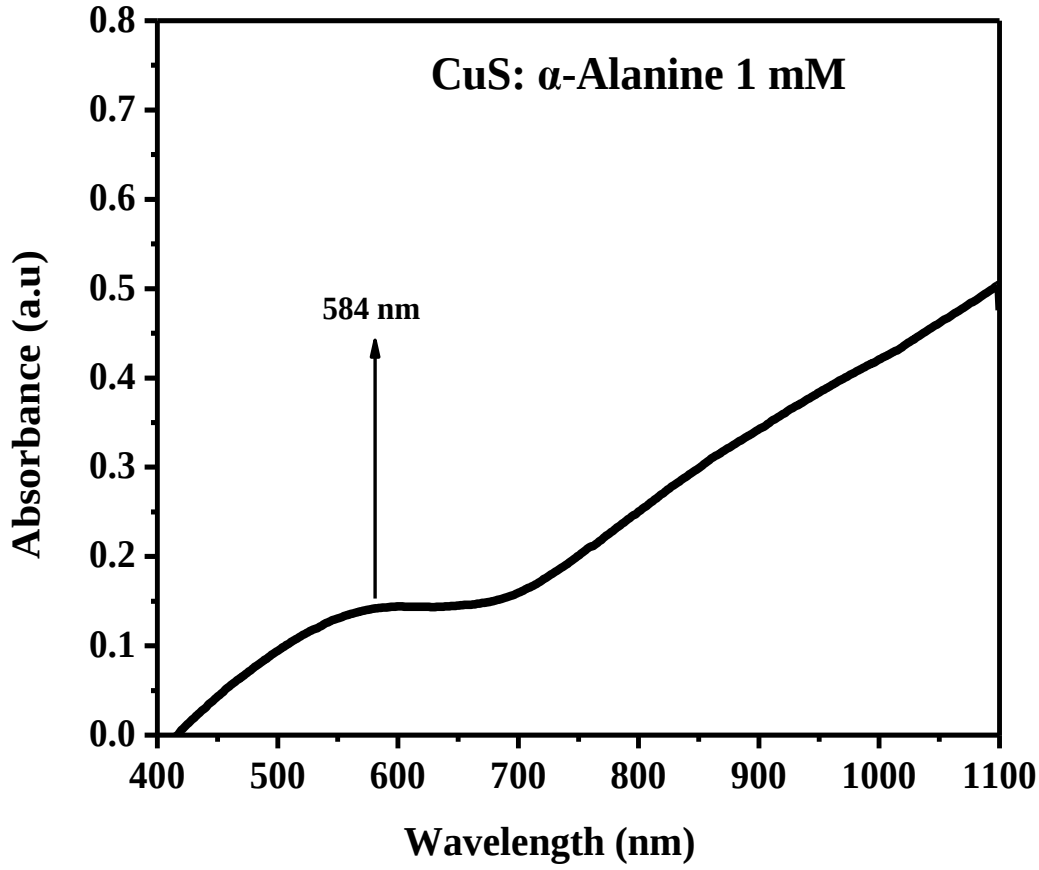

Figure 3.6 UV-Visible spectrum of CuS Nanorods using I mM of α-Alanine.

3.1.5.1 Comparison of UV-Visible spectra

In all the UV-Visible Spectra of CuS nanorods by using different concentration of capping agent have maximum absorbance beyond the 1100 nm due to the smaller band gap. The sample synthesized by using I1 mM of α-Alanine shows the blue shift at lower wavelength as compared by using the 1 mM of α-Alanine. This blue shift at lower wavelength indicates the decrease in size of CuS nanomaterials. UV-Visible absorption spectrum of CuS nanorods in water solvent was measured at the wavelength range of 200-1100 nm. In the visible region an absorption peak is appeared at around 572 nm. This peak has very broad absorption which is due to electronic transition from valence band of CuS to first conduction band. The broadness shows that presence of the various surface energy states between valence and conduction bands of CuS. Peak appear at 572 nm is less sharp. This less sharpness shows that the presence of various surface energy state between valence and conduction band of CuS. Due to very wide absorption window, this is good material for the application in solar cell.

The UV-Visible Spectrum of CuS nanorods by using 21 mM of α-Alanine also give the absorption peak in visible region at 521 nm. This peak has broad absorption which is due to the electronic transition from valence band of CuS to first conduction band. The less sharpness of peak at 521 nm showed that there is various energy surface states present between valence and conduction band of CuS. Due to very wide absorption window it is good material for solar cell. This sample also shows the blue shift at lower wavelength as compare to all previous absorption spectra. It is the indication of reduction in size by increasing the concentration of capping agent.

The next one UV-Visible Spectrum of CuS nanorods is synthesized by using 31 mM of α-Alanine. In this sample one absorption peak which is appeared in the visible region shows the blue shift. The UV-Visible absorption spectrum of the CuS nanorods in water solvent was measured at the wavelength range of 200-1100 nm. An absorption peak in visible region at 500 nm is appeared and maximum absorption of the CuS nanorods occurs beyond the 1100 nm. Due to the very wide absorption window, this is also very good material for the application in solar cell. The peak at 500 nm has broad absorption due to the electronic transition from valence band of CuS to first conduction band. This broadness is due to various energy surface states which are present between valence and conduction band of CuS. This less sharpness of peak at 500 nm showed that there is also various surface energy states present between valence and conduction band of the CuS.

UV-Visible Spectrum of CuS nanorods synthesized by using 51 mM of α-Alanine show that blue shift which is the sign of decrease in size of required material. The maximum absorption of CuS nanoparticle is beyond the 1100 nm. Due to the very wide absorption window of CuS, it is very good material for the application in solar cell. The UV-Visible absorption spectrum of CuS nanorods was measured in the water solvent at the wavelength range of 200-1100 nm. In visible region an absorption peak is appeared at around 472 nm. This peak has broad absorption which is due to the electronic transition from valence band of CuS to first conduction band. The broadness is due to various surface energy states which are present between valence and conduction band of the CuS.

All UV-Visible absorption spectra also showed a blue shift in all the absorption spectra at by increasing the concentration of capping agent (α-Alanine). The comparison of all UV-Visible absorption spectra are given below in the figure 3.7 in which absorption wavelength data showed that the blue shift was generated by lesser size nanoparticles and the red shift by larger size nanoparticles. By increasing the concentration of capping agent (α-Alanine) blue shift was observed towards the lower

wavelength. The absorption spectra proposed by increasing the concentration of α-Alanine blue shifted and broader absorption occurred, which is the indication of decrease in size of CuS nanorods.

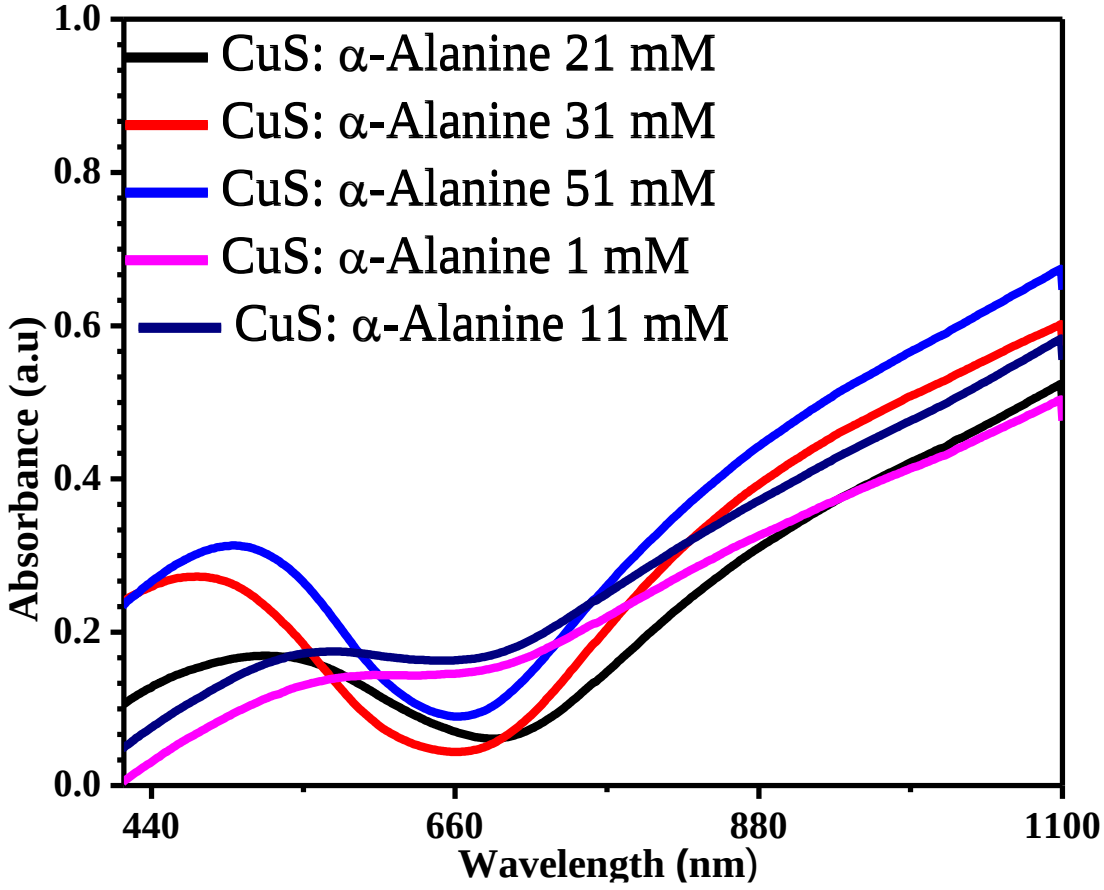

Figure 3.7 UV-Visible spectra of CuS Nanorods using different concentration of α-Alanine.

3.1.6 PL Spectrum of CuS Nanorods Using 1 mM of α-Alanine

Photoluminescence spectroscopy is utilized to measure fluorescence excitation and emission in the molecules and substances. Photoluminescence (PL) spectroscopy is the major technique for the determination of the optical properties of nanoparticles. The excitation wavelength for all the photoluminescence spectra of CuS nanorods is 290 nm in this thesis. The Emission wavelength data showed that the blue shift was created by smaller size nanoparticles and red shift by greater size nanoparticles.

The photoluminescence spectrum of CuS nanorods synthesized by using 1 mM of α-Alanine is given in the figure 3.8. This spectrum shows that there are two different emissive peaks in the UV and visible region at the wavelength 323 nm and 422 nm. The peak appeared at 420 nm is broader as compare to the other peak at 323 nm. The broader

emissive peak having the long decay and this shows that the presence of more surface energy states. The peak in the UV region is appeared due to the de-excitation from higher conduction band to valence band of CuS nanorods. Less broadness shows that there are no any energy surface state is present. The peak in the visible region is very broad emissive and shows that the de-excitation of the electron from first conduction band to the valence band of CuS. Mostly the broadness is due to the large number of energy surface states which are present in the CuS first conduction band and valence band.

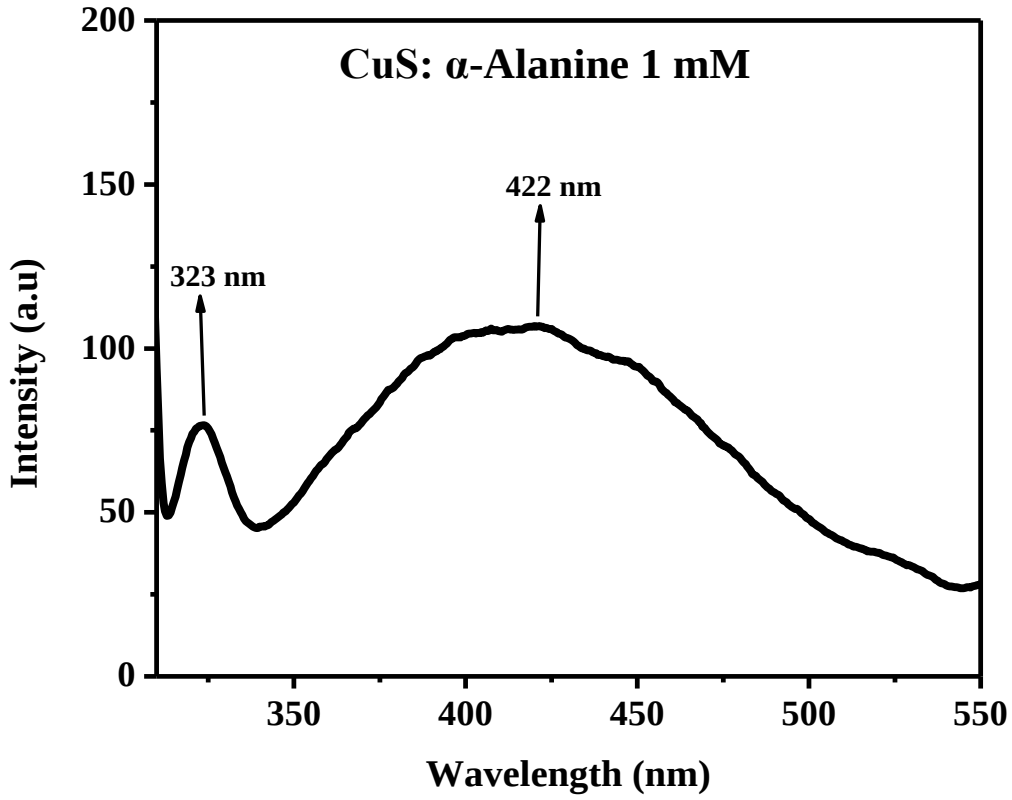

Figure 3.8 PL Spectrum of CuS Nanorods using 1 mM of α-Alanine

3.1.6.1 Comparison of Photoluminescence spectra

The Photoluminescence spectrum of CuS nanorods synthesized by using 11 mM of α-Alanine has two different emissive peaks in the UV and visible region at the wavelength 324 nm and 417 nm. The peak appeared at 417 nm is broader as compare to the other peak at 324 nm. The peak in the UV region is appeared due to the de-excitation from higher conduction band to valence band of CuS and less broadness shows that there are no any surface energy state is present. The peak in the visible region is very broad emissive which is due to the large number of surface energy states which are present in

the CuS first conduction band and valence band. In this sample the peak appeared at 417 nm is broader as compare to the peak appeared at 422 nm in the case of synthesized CuS nanorods by using the 1 mM of α-Alanine. This broadening of the peak in sample of 11 mM of α-Alanine shows that by increasing the concentration of capping agent the blue shift occurs at the lower wavelength. The intensity of the broadening peak is also decreased in sample of 11 mM of α-Alanine.

The CuS nanorods sample formed by using the 21 mM of α-Alanine also shows the two distinctly different emissive peaks which appeared in the UV and visible region at wavelength 323 nm and 415 nm respectively. Peak which appeared in visible region is due to de-excitation of electrons from first conduction band of CuS to the valence shell and is broader emissive peak. This broadness is due to the many number of surface energy state which are present between first conduction band and the valence band of nanomaterials. The peak which is appeared in the UV region is due to de-excitation of the electrons from higher conduction band of CuS to valence band. The appeared in the visible region is broader as compare to the peak at 323 nm. Similarly this peak is broader as contrast to the peak at 422 nm in the case of 1 mM of α-Alanine. This broadening shows that the CuS nanorods have less size as compare to the synthesized CuS nanorods by using the 1 mM of α-Alanine. By analysis of this PL spectrum we can say that by increasing the concentration of α-Alanine the blue shift occur at lower wavelength which is the sign in reduction of size in our synthesized nanomaterials.

Photoluminescence spectrum of CuS nanorods synthesized by using 31 mM of α-Alanine also shows two peaks. It is a non-destructive way of probing the optical properties of a material. By using 31 mM of α-Alanine we synthesized CuS nanorods which have two different emissive peaks at the wavelength 324 nm and 411 nm. The peak at 411 nm is broader as compare to that peak which has appeared at 324 nm. Peak which appeared at 324 nm is due to the de-excitation from higher conduction band to valence band of CuS and less broadness shows that there are no any energy surface state is present. The peak at 411 nm is very broad emissive and shows that the de-excitation of electron from first conduction band to valence band of CuS. Mostly the broadness is due to the large number of energy surface states which are present in the CuS first conduction band and valence band. On comparing this sample with CuS nanorods formed by using 1 mM of α-Alanine we get broader peak at wavelength 411 nm in this sample. This broadening shows that there is further reduction in the size of CuS nanorods. We can say

that by increasing the concentration of capping agent we observed decrease in the size and blue shift at lower wavelength.

CuS nanorods which are synthesized by using the 41 mM of α-Alanine. Photoluminescence spectrum of CuS nanorods formed by using 41 mM of α-Alanine shows that there are two different emissive peaks at wavelength 326 nm and 376 nm. On comparing this sample and sample of CuS nanorods which is formed by using the 1 mM α-Alanine we get result that blue shift appeared at lower wavelength. The peak appeared at 376 nm is broader as compare to the peak appeared at 326 nm. The peak at 326 nm appeared due to the de-excitation from the higher conduction band to valence band of the CuS and less broadness shows that there are no any energy surface state is present. The peak at 376 nm is very broad emissive and shows that the de-excitation of the electron through first conduction band to the valence band of CuS. Mostly the broadness is due to the large number of energy surface states which are present in the CuS first conduction band and valence band.

On comparing sample of CuS nanorods synthesized by using 51 mM of α-Alanine and sample of CuS nanorods which is formed by using the 1 mM α-Alanine we get result that blue shift appeared at lower wavelength. Blue shift at lower wavelength is the indication of decrease in the size of CuS nanorods .The CuS nanorods sample formed by using the 51 mM of α-Alanine also shows the two distinctly different emissive peaks which appeared in the UV at the wavelength 325 nm and 380 nm. The peak at 380 nm is broader as compare to the peak appeared at 325 nm. The peak at 325 nm due to the de-excitation from the higher conduction band to valence band of the CuS and less broadness shows that there are no any energy surface state is present. The peak at 380 nm is very broad emissive which is due to de-excitation of the electron from first conduction band to the valence band of CuS. The broadening of peak is more and more at the higher concentration of α-Alanine.

The photoluminescence spectroscopy is the principal technique for the determination of the optical properties of nanorods. Comparison of all photoluminescence spectra with excitation wavelength 290 nm are given below in the figure 3.9 in which emission wavelength data showed that the blue shift was generated by lesser size CuS nanorods and the red shift by larger size CuS nanorods. By increasing the concentration of capping agent (α-Alanine) blue shift was observed towards lower wavelength. The photoluminescence spectra suggested by increasing the concentration of α-Alanine blue

shifted and broader emission occurred, which is also an indication of decrease in size of CuS nanorods.

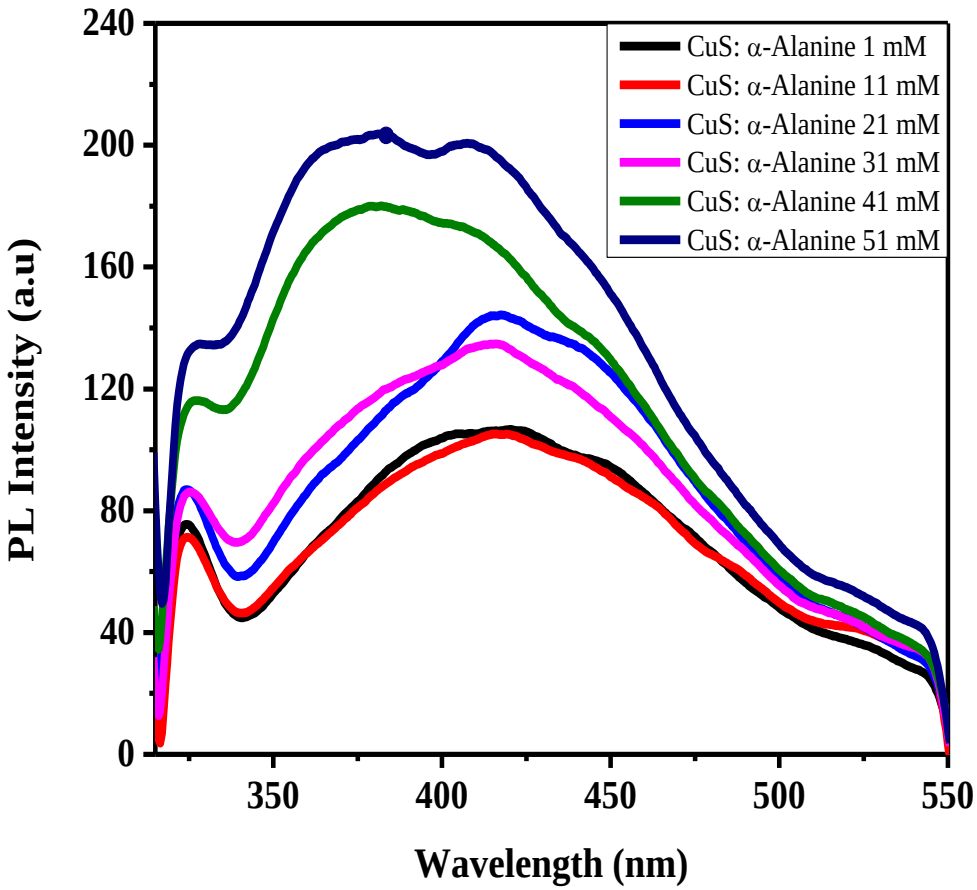

Figure 3.9 PL Spectra of CuS Nanorods using different concentration of α-Alanine.

3.2 C-V measurement of Nanorods Synthesized Solar Cell

Current voltage (I-V) measurement of CuS nanorods was carried out by using solar simulator. I-V graph is shown in the figure 3.10. CuS nanorods synthesized by using 51 mM of α-Alanine showed large open circuit voltage (Voc) and short circuit current (Jsc) as compared to nanorods synthesized by using I mM of α-Alanine. The fill factor is slightly greater in the case of 51 mM of α-Alanine. This increase in Jsc shows that the overall exciton life time increased as result the chance to reach at CuS nanorods interface increases and more charge carrier produces. So due to the greater number of charge carrier the short circuit current increases from 0.00258 Acm^{-2} to 0.00273 Acm^{-2}. The open circuit voltage also increases from 0.77 V to 0.79 V by using the 51 mM of α-Alanine.

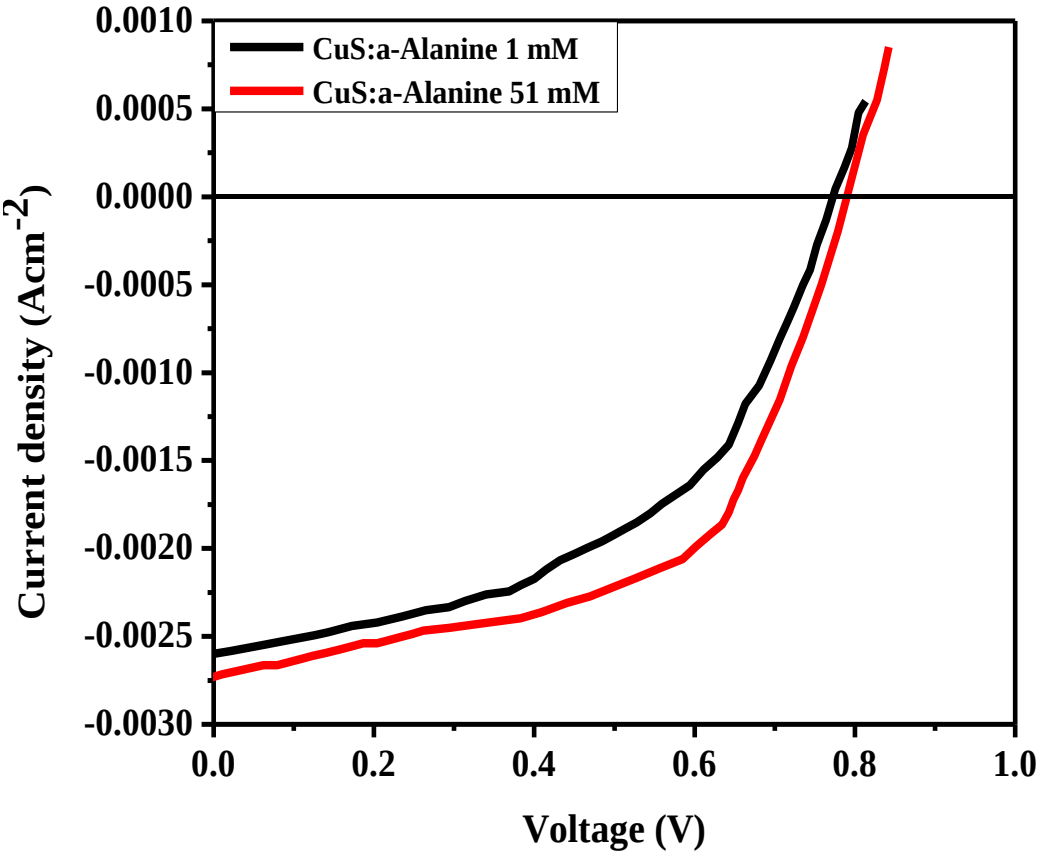

Figure 3.10 I-V measurement of nanorods synthesized solar cell

3.2.1 C-V measurement calculation of nanorods Synthesized Solar Cell

Efficiency calculation are shown in the table 3.2.The fill factor value and efficiency were calculated by using the following given formulas.

$$FF = \frac{I_{MPP} \cdot V_{MPP}}{I_{sc} \cdot V_{oc}}$$

$$\eta(\%) = \frac{V_{oc} \times J_{sc} \times \mathrm{FF}}{P_{in}}$$

$$P_{in} = 100\ \mathrm{mWcm^{-2}}$$

Table 3.3 I-V measurement calculation for nanorods solar cell.

Sr.No.	J_{sc} (A cm^{-2})	V_{oc} (v)	F.F	Efficiency (%)
CuS: α-Alanine 1 mM	0.00258	0.77	0.49	0.97
CuS: α-Alanine 51 mM	0.00273	0.79	0.55	1.2

Efficiency (%) calculated by using above formula for CuS: α-Alanine 1 mM is 0.97 and for CuS: α-Alanine 51 mM is 1.2. The fill factor value of CuS: α-Alanine 51 mM is slightly greater as compare to CuS: α-Alanine 1 mM.

Conclusions

CuS nanorods were synthesized and its synthesis was confirmed by elemental analysis, XRD and SEM techniques. Elemental analysis also confirmed the presence of Cu and S in the nanorods with atomic and weight percentages.

CuS nanorods were successfully synthesized and their confirmation was done by FTIR measurements, where a characteristics peak of CuS at wave number 609 cm^{-1} had been observed. XRD patterns suggested that CuS nanorods were grown in hexagonal crystal structure and by increasing the concentration of α-Alanine the size was decreased. Crystallite size calculated from XRD analysis was 15.6 nm. XRD analysis revealed that nanorods are highly crystalline nature with the hexagonal crystal structure. SEM images suggested that the CuS nanorods have been agglomerated and appeared in the form of rod shape in the given SEM images resolution. SEM results showed the formation of nanorods with size of 80-95 nm. UV-Visible absorption spectrum also showed a blue shift in the absorption spectra by increasing the concentration of α-Alanine. These observations were in consistent with XRD measurements. Optical studies by UV-Vis spectroscopy revealed that it had wide absorption window. Photoluminescence spectra suggested by increasing the concentration of α-Alanine blue shifted and broader emission occurred, which is also an indication of decrease in size of CuS Nanorods. The photoluminescence (PL) spectra showed that CuS nanorods emit in both UV and visible regions. The current-voltage measurements of CuS: α-Alanine 51 mM gave large J_{sc} and F.F as compared to CuS: α-Alanine 1 mM. The Jsc calculated for CuS: α-Alanine 51 mM and CuS: α-Alanine 1 mM is 0.00273 Acm^{-2} and 0.00258 Acm^{-2}, and the corresponding efficiencies (%) are 1.2 and 0.97 respectively.

Future Work

- To study the effect of different capping agents on size of CuS nanorods.
- To study the effect of temperature and pH on size of CuS nanorods.
- The applications of CuS nanorods in photodiodes, phototransistors, gas sensors, fuel cell, transparent electrode, batteries and in biomedical field such as treatment of cancer cell.
- To check their capability as a solar cell.

References

(1) Bhushan, B. Handbook of Nanotechnology; Springer, **2004**, 6, 497-516.

(2) Bainbridge, W. S.; Roco, M. C. Managing nano-bio-info-cogno innovations; Springer, **2006**, 2, 153-171.

(3) Huang, C.; Notten, A.; Rasters, N. J. Technol. Transfer **2011**, 36, 145-172

(4) Park, K. J. Controlled Release Soc. **2007**, 120, 1-3

(5) Utsav, M. Int. J. Appl. Phys. Math. **2014**, 4, 51-54.

(6) Guo, Y.; Huang, L.; Porter, A. L. Nano. Lett. **2010**, 16, 361-374.

(7) Chu, Y. Int. J. Appl. Phys **2011**, 22, 318-331.

(8) Kuchibhatla, S. V.; Karakoti, A.; Bera, D.; Seal, S. Prog. Mater. Sci. **2007**, 52, 699-913.

(9) Bera, D.; Kuiry, S. C.; Seal, S. Jom, Nano. Lett. **2004**, 56, 49-53.

(10) Bera, D.; Qian, L.; Tseng, T.-K.; Holloway, P. H. J. Mater. Sci. **2010**, 3, 2260-2345.

(11) Phaal, R. Nano. Lett. **2011**, 6, 19-25.

(12) Bronicki, L. Y.; Berger, D. Eur. Phy. J. C **2014**, 12, 23-31.

(13) El Kurdi, M.; Prost, M.; Ghrib, A.; Sauvage, S.; Checoury, X.; Beaudoin, G.; Sagnes, I.; Picardi, G.; Ossikovski, R.; Boucaud, P. ACS Photonics **2016**, 3, 443-448.

(14) Liu, J.; Sun, X.; Pan, D.; Wang, X.; Kimerling, L. C.; Koch, T. L.; Michel, J. Opt. Express **2007**, 15, 11272-112777.

(15) Huo, Y.; Lin, H.; Chen, R.; Makarova, M.; Rong, Y.; Li, M.; Kamins, T. I.; Vuckovic, J.; Harris, J. S. Appl. Phys. Lett. **2011**, 98, 1866-1868

(16) Sánchez-Pérez, J. R.; Boztug, C.; Chen, F.; Sudradjat, F. F.; Paskiewicz, D. M.; Jacobson, R.; Lagally, M. G.; Paiella, R. Proc. National Acad. Sci. **2011**, 108, 18893-18893.

(17) Boztug, C.; Sánchez-Pérez, J. R.; Cavallo, F.; Lagally, M. G.; Paiella, R. ACS. Nano. **2014**, 8, 3136-3151.

(18) Sukhdeo, D. S.; Nam, D.; Kang, J.-H.; Brongersma, M. L.; Saraswat, K. C. Photonics Res. **2014**, 2, 8-13.

(19) Gallagher, J.; Xu, C.; Jiang, L.; Kouvetakis, J.; Menéndez, J. Appl. Phys. Lett. **2013**, 103, 202104-202124.

(20) Gupta, S.; Magyari-Köpe, B.; Nishi, Y.; Saraswat, K. C. J. Appl. Phys.**2013**, 113, 73707-73717.

(21) Wirths, S.; Geiger, R.; Von Den Driesch, N.; Mussler, G.; Stoica, T.; Mantl, S.; Ikonic, Z.; Luysberg, M.; Chiussi, S.; Hartmann, J. Nat. Photonics **2015**, 9, 88-92.

(22) Betts, M. J.; Russell, R. B. J. Appl. Phys. Lett. **2007**, 2, 311-342.

(23) Davies, J. S. Amino Acids, Pept. Proteins; R. Soc. Chem. **1998**, 29,13-21.

(24) Rozenberg, M.; Shoham, G.; Reva, I.; Fausto, R. Spectrochimica Acta Part A: Mol. Biomol. Spectrosc. **2003**, 59, 3253-3266.

(25) Barthes, M.; Vik, A. F.; Spire, A.; Bordallo, H. N.; Eckert, J. Phys. Chem. A **2002**, 106, 5230-5241.

(26) Betts, M. J.; Russell, R. B. J. Dispersion Sci. Technol. **2003**, 317, 289-298.

(27) Peart, D. J.; Kirk, R. J.; Madden, L. A.; Vince, R. V. Amino acids **2016**, 48, 499-504.

(28) Balabin, R. M. J. Phys. Chem. **2010**, 12, 5980-5982.

(29) Hirata, Y.; Kubota, S.; Watanabe, S.; Momose, T.; Kawaguchi, K. J. Mol. Spectrosc. **2008**, 251, 314-318.

(30) Gibson, B. Sol. Energy Mater. Sol. Cells **2011**, 12, 24-28.

(31) Nelwamondo, S.; Moloto, M.; Krause, R.; Moloto, N. Mater. Lett. **2012**, 75, 161-164.

(32) Singh, K. V.; Martinez-Morales, A. A.; Andavan, G. S.; Bozhilov, K. N.; Ozkan, M. Chem. Mater. **2007**, 19, 2446-2454.

(33) Zou, J.; Zhang, J.; Zhang, B.; Zhao, P.; Xu, X.; Chen, J.; Huang, K. J. Mater. Sci. **2007**, 42, 9181-9186.

(34) Devi, B. R.; Raveendran, R.; Vaidyan, A. Mater. Sol. Cells **2007**, 68, 679-687.

(35) Gautam, U. K.; Mukherjee, B. Bull. Mater. Sci. **2006**, 29, 1-5.

(36) Brelle, M.; Torres-Martinez, C.; McNulty, J.; Mehra, R.; Zhang, J. Pure Appl. Chem. **2000**, 72, 101-117.

(37) Alsema, E.; de Wild-Scholten, M.; Fthenakis, V. Eur. Phy. J. B **2006**, 320, 14-17.

(38) Carotenuto, G.; Capezzuto, F.; Palomba, M.; Nicolais, F. Int. J. Nanosci. **2010**, 9, 385-389.

(39) Baláž, P.; Takacs, L.; Boldižárová, E.; Godočíková, E. J. Phys. Chem. Solids **2003**, 64, 1413-1417.

(40) Boey, H.; Tan, W.; Bakar, N. A.; Bakar, M. A.; Ismail, J. Phys. Sci. **2007**, 18, 87-101.

(41) Li, F.; Bi, W.; Kong, T.; Qin, Q. Crystal Res. Technol. **2009**, 44, 729-735.

(42) Hagfeldt, A.; Graetzel, M. Chem. Rev. **1995**, 95, 49-68.

(43) Priaulx, M. J. Mater. Sci. Technol. **2005**, 24, 195-225

(44) Gonçalves, L. M.; de Zea Bermudez, V.; Ribeiro, H. A.; Mendes, A. M. Energ. Environ. Sci. **2008**, 1, 655-668.

(45) Milliron, D. J.; Gur, I.; Alivisatos, A. P. J. Photoch. Photobiol. **2005**, 30, 136-150.

(46) Sharma, S.; Jain, K. K.; Sharma, A. Mater. Sci. Appl. **2015**, 6, 1145-155

(47) Cai, W.; Gong, X.; Cao, Y. Sol. Energ. Mat. Sol. C **2010**, 94, 114-127.

(48) Srinivas, B.; Balaji, S.; Nagendra Babu, M.; Reddy, Y. Int. J. Eng. Res. Online **2015**, 3, 178-189.

(49) Etgar, L. Mater. Eng. **2013**, 6, 445-559.

(50) Fraas, L. M. Energ. Fuel **2014**, 113, 1717-1730.

(51) Gibson, B. Sol. Energ. **2011**, 12, 532-538.

(52) Bagher, A. M.; Vahid, M. M. A.; Mohsen, M. Am. J. Opt. Photonics **2015**, 3, 94-113.

(53) Shruti Sharma, Kamlesh Kumar Jain, Ashutosh Sharma,1CMD College, Bilaspur, India, University of Seoul, Seoul, South Korea, Mater. Sci. Appl. **2015**, 6, 1145-1155.

(54) Choubey, P.; Oudhia, A.; Dewangan, R. Recent Res. Sci. Technol. **2012**, 4, 99-10

(55) Chopra, K.; Paulson, P.; Dutta, V. Prog. Photovoltaics Res. Appl. **2004**, 12, 69-92.

(56) Heywang, W.; Zaininger, K. In Silicon; Springer: **2004**, 4, 25-42.

(57) Zaharia, Kopidakis, N.; Olson, D. C.; Ginley, Int. J. Nanosci. **2013**, 3, 365-383.

(58) Brabec, C. J. Sol. Energ. Mater. Sol. Cells **2004**, 83, 273-292.

(59) Chen, Q.; Zhou, H.; Hong, Z.; Luo, S.; Duan, H.-S.; Wang, H.-H.; Liu, Y.; Li, G.; Yang, Y. J. Am. Chem. Soc. **2013**, 136, 622-625.

(60) Sjöholm, K. H.; Rasmussen, M.; Minteer, S. D. ECS Electrochem. Lett. **2012**, 1, 7-9.

(61) Sofos, M.; Goldberger, J.; Stone, D. A.; Allen, J. E.; Ma, Q.; Herman, D. J.; Tsai, W.-W.; Lauhon, L. J.; Stupp, S. I. Nat. Mater. **2009**, 8, 68-75

(62) Fitra, M.; Daut, I.; Gomesh, N.; Irwanto, M.; Irwan, Y. Energ. Proc. **2013**, 36, 341-348.

(63) Ludin, N. A.; Mahmoud, A. A.-A.; Mohamad, A. B.; Kadhum, A. A. H.; Sopian, K.; Karim, N. S. A. Renew. Sustainable Energ. Rev. **2014**, 31, 386-396.

(64) Jeong, J.-A.; Kim, H.-K. Sol. Energ. Mater. Sol. Cells **2011**, 95, 344-348.

(65) Artemyev, M. V.; Woggon, U.; Wannemacher, R.; Jaschinski, H.; Langbein, W. Nano. Lett. **2001**, 1, 309-314.

(66) Graham-Rowe, D. Nat. Photonics **2009**, 3, 307-309.

(67) Coe-Sullivan, S. Nat. Photonics **2009**, 3, 315-316.

(68) Petrov, D.; Santos, B.; Pereira, G.; de Mello Donegá, C. J. Phys. Chem. B **2002**, 106, 5325-5334.

(69) Bailey, R. E.; Nie, S. J. Am. Chem. Soc. **2003**, 125, 7100-7106.

(70) Zhong, X.; Han, M.; Dong, Z.; White, T. J.; Knoll, W. J. Am. Chem. Soc. **2003**, 125, 8589-94.

(71) Gurusinghe, N. P.; Hewa-Kasakarage, N. N.; Zamkov, M. J. Phys. Chem. C **2008**, 112, 12795-12800.

(72) Korgel, B. A.; Monbouquette, H. G. Langmuir **2000**, 16, 3588-3594.

(73) Harrison, M.; Kershaw, S.; Burt, M.; Eychmüller, A.; Weller, H.; Rogach, A. Mater. Sci. Eng. B **2000**, 69, 355-360.

(74) Lee, H.; Holloway, P. H.; Yang, H. J. Chem. Phys. **2006**, 125, 164711-164717.

(75) Zhong, X.; Feng, Y.; Knoll, W.; Han, M. J. Am. Chem. Soc. **2003**, 125, 13559-13563.

(76) Ewald, P. P. Aip. Conf. Proc. **1962**, 17, 45-47.